Mathematics

https://www.aimspress.com/journal/Math

AIMS Mathematics, 11(7): 20956–20985.
DOI: 10.3934/math.2026851
Received: 27 April 2026
Revised: 05 July 2026
Accepted: 10 July 2026
Published: 16 July 2026

Research article

Novel solutions and stability analysis for the (3+1)-dimensional B-type Kadomtsev–Petviashvili equation using an improved generalized Riccati equation mapping technique

Noha M. Kamel[1,*], Hamdy M. Ahmed[2] and Wafaa B. Rabie[3]

[1] Department of Physics and Engineering Mathematics, Faculty of Engineering, Ain Shams University, Cairo, Egypt
[2] Department of Physics and Engineering Mathematics, Higher Institute of Engineering, El-Shorouk Academy, Cairo, Egypt
[3] Department of Mathematics, Faculty of Science, Luxor University, Taiba Luxor, Egypt

* **Correspondence:** Email: noha.medhat@eng.asu.edu.eg.

Abstract: This study retrieved novel abundant exact solutions for the (3+1)-dimensional B-type Kadomtsev–Petviashvili equation using the improved generalized Riccati equation mapping technique. The B-type Kadomtsev–Petviashvili equation is of high importance in modeling nonlinear wave propagation in weakly dispersive media in fluid dynamics and plasmas. The derived solutions included singular, bright, and bright-dark solitons, as well as hyperbolic, rational, exponential, and singular periodic solutions. The validation of the derived solutions was confirmed by direct substitution into the B-type Kadomtsev–Petviashvili equation under study. A detailed stability analysis was performed utilizing the linear stability analysis concept. The obtained stability results indicated the presence of neutral stability and the non-existence of modulation instability for any choice of the system parameters. The wave dynamics of some derived exact solutions are illustrated by two-dimensional, three-dimensional, and density plot graphics. Additionally, the results of stability analysis are illustrated by two-dimensional and three-dimensional graphics.

Keywords: (3+1)-dimensional B-type Kadomtsev–Petviashvili equation; improved generalized Riccati equation mapping technique; stability analysis; graphical illustrations
Mathematics Subject Classification: 35C07, 35C08, 35C09

1. Introduction

Nonlinear evolution equations (NEEs) are a kind of nonlinear partial differential equations (NPDEs) with time as one of the independent variables. NEEs are considered as crucial models in the analysis of physical phenomena and in studying dynamical behavior in labs [1–3]. A well-known NEE is the KdV equation, which was introduced in 1895 by the scientists Korteweg and de Vries, initially used to model surface waves, in shallow water, having long wavelength and small amplitude [4–6]. Different forms of the KdV equation are now used to model water wave propagation and plasma waves in fluid mechanics [7–9]. The well-known Kadomtsev–Petviashvili equation (KPE) is another NEE, which extended the KdV equation to two-dimensions, introduced by Kadomtsev and Petviashvili in 1970 to model shallow water surface waves with small amplitude under weak disturbances [10]. The KPE-hierarchy is defined as the modified or extended forms of the KPE [11], and has been used in many fields such as plasma physics [12,13], quantum mechanics [14,15], neural networks [16,17], nonlinear optics, and fluid dynamics [18–20].

The KPE hierarchy is divided into sub-hierarchies. For example, in [21], a sub-hierarchy called "A-type KPE" was defined, associated with the A-type infinite dimensional Lie algebra. In [22,23], a sub-hierarchy called "B-type KPE" was defined, related to the B-type infinite dimensional Lie algebra [24]. The following (2+1)-dimensional B-type Kadomtsev–Petviashvili equation (BKPE) was first discussed in [22]:

$$\begin{aligned}&\frac{\partial u}{\partial t}-5\left(\frac{\partial^3 u}{\partial y\,\partial x^2}+\int\frac{\partial^2 u}{\partial y^2}\,dx\right)+\frac{\partial^5 u}{\partial x^5}+15\left(\frac{\partial u}{\partial x}\frac{\partial^2 u}{\partial x^2}+u\,\frac{\partial^3 u}{\partial x^3}-u\,\frac{\partial u}{\partial y}-\frac{\partial u}{\partial x}\int\frac{\partial u}{\partial y}\,dx\right)\\&+45\,u^2\,\frac{\partial u}{\partial x}=0,\end{aligned}\tag{1.1}$$

which has been extensively applied in quasi media [25–27] and fluid mechanics [28–30] to model weakly dispersive wave propagation. For years, researchers have been focusing on the following (3+1)-dimensional BKPE [31] to model weakly dispersive wave propagation in fluid dynamics:

$$\begin{aligned}&\frac{\partial u}{\partial t}-5\left(\frac{\partial^3 u}{\partial y\,\partial x^2}+\int\frac{\partial^2 u}{\partial y^2}\,dx\right)+\frac{\partial^5 u}{\partial x^5}+15\left(\frac{\partial u}{\partial x}\frac{\partial^2 u}{\partial x^2}+u\,\frac{\partial^3 u}{\partial x^3}-u\,\frac{\partial u}{\partial y}-\frac{\partial u}{\partial x}\int\frac{\partial u}{\partial y}\,dx\right)\\&+45\,u^2\,\frac{\partial u}{\partial x}+\alpha\,\frac{\partial u}{\partial z}=0.\end{aligned}\tag{1.2}$$

Different exact solutions for Eq (1.2) have been obtained, such as periodic solutions by applying a combination of Hirota bilinear method and Riemann theta functions in [32]. In [33], breather solutions were found by combining Hirota bilinear and complexification methods, while rogue and lump solutions were obtained in [34] using Hirota method and many more [1,35,36]. In [37], Wazwaz suggested the following new extended (3+1)-dimensional B-type Kadomtsev-Petviashvili equation:

$$\begin{aligned}&9\frac{\partial u}{\partial t}-5\left(\frac{\partial^3 u}{\partial y\,\partial x^2}+\int\frac{\partial^2 u}{\partial y^2}\,dx\right)+\frac{\partial^5 u}{\partial x^5}+15\left(\frac{\partial u}{\partial x}\frac{\partial^2 u}{\partial x^2}+u\,\frac{\partial^3 u}{\partial x^3}-u\,\frac{\partial u}{\partial y}-\frac{\partial u}{\partial x}\int\frac{\partial u}{\partial y}\,dx\right)\\&+45\,u^2\,\frac{\partial u}{\partial x}+\alpha\,\frac{\partial u}{\partial x}+\beta\,\frac{\partial u}{\partial y}+\gamma\,\frac{\partial u}{\partial z}=0,\end{aligned}\tag{1.3}$$

which, by the substitution

$$u=\frac{\partial q}{\partial x},\tag{1.4}$$

is transformed to

$$
\begin{aligned}
&9\frac{\partial^2 q}{\partial t\,\partial x}-5\left(\frac{\partial^4 q}{\partial y\,\partial x^3}+\frac{\partial^2 q}{\partial y^2}\right)+\frac{\partial^6 q}{\partial x^6}+\ 15\left(\frac{\partial^2 q}{\partial x^2}\frac{\partial^3 q}{\partial x^3}+\frac{\partial q}{\partial x}\frac{\partial^4 q}{\partial x^4}-\frac{\partial q}{\partial x}\frac{\partial^2 q}{\partial y\,\partial x}-\frac{\partial^2 q}{\partial x^2}\frac{\partial q}{\partial y}\right)\\
&+45\left(\frac{\partial q}{\partial x}\right)^2\frac{\partial^2 q}{\partial x^2}+\alpha\,\frac{\partial^2 q}{\partial x^2}+\beta\,\frac{\partial^2 q}{\partial y\,\partial x}+\gamma\,\frac{\partial^2 q}{\partial z\,\partial x}=0,
\end{aligned}
\tag{1.5}
$$

where α, β, and γ are arbitrary constants. The function $q(x, y, z, t)$ measures the wave's amplitude; t, and x, y, z, are the temporal and spatial dimensions, respectively.

1.1. Comparison of this work with previous work in literature

Wazwaz [37] showed that Eq (1.5) is Painlevé integrable and explored multiple soliton, lump, and breather solutions using Hirota's and ansatz methods. According to our knowledge, only two works discussed Eq (1.3) since its first appearance. The first [38] investigated Eq (1.5) using the generalized Kudryashov method and the unified method. The second [39] investigated Eq (1.5) using the Hirota bilinear method.

In this study, the improved generalized Riccati equation mapping (IGREM) technique [40] is applied to derive abundant novel exact solutions for Eq (1.3). The first novelty of this study is the application of new technique, the IGREM technique, to Eq (1.5) for the first time. The IGREM technique has great potential in the analytical solution of different types of NLPDEs. Its advantages include easy application, direct calculations, and abundant forms of exact solutions that can be generated by symbolic computation [41]. These advantages encouraged the application of the IGREM technique to a wide range of NPDEs, as shown in the literature, such as the (3+1)-dimensional Jimbo–Miwa equation [42], the (3+1)-dimensional Kadomtsev–Petviashvili–Sawada–Kotera–Ramani equation [43], and many other NPDEs [44, 45].

The second novelty is the retrieval of abundant novel exact solutions for Eq (1.3), such as singular, bright, and bright-dark solitons, as well as hyperbolic, rational, exponential, and singular periodic solutions for the first time in the literature, (see Table 1). Some of the obtained solutions, in this work and previous works in the literature, are complex-valued, which have great importance in complex-valued physical problems such as quantum mechanics, optical fibers, and fluid dynamics where solutions are of complex type. In optical fiber communications, complex-valued solutions sharpen models of pulse propagation under dispersion and nonlinearity, thus optimizing high-speed data transmission. Complex-valued wave solutions are important in shallow water because they provide a powerful analysis of the wave dynamics, particularly regarding energy dissipation, phase shifts, and wave scattering. They are essential for understanding nonlinear phenomena and modeling complex coastal phenomena such as rogue waves [46, 47].

The third novelty is the visual illustration of derived solutions of Eq (1.3) with 2D, 3D, and density plots for the first time in the literature, (see Table 1). This work presents a detailed stability analysis for Eq (1.5), whose the graphical illustration is visualized by 2D and 3D plots for the first time in the literature, which makes up the fourth novelty. The details of the verification of obtained solutions, by direct substitution into the original equation and turning it into identity, are also presented.

Table 1 presents a comparison between this work and previous work related to Eq (1.3). The application of only the IGREM technique to Eq (1.5) retrieved many more different forms of exact solutions than those obtained by two or more methods in any previous works.

Table 1. Comparison of the outputs of this work and previous works available in the literature

Article Ref. No.	Applied techniques	Derived exact solutions $q(x, y, z, t)$ for the transformed equation in Eq (1.5), and $u(x, y, z, t)$ for the investigated BKPE in Eq (1.3)	Analytic expressions of $u(x, y, z, t)$	Graphics of $u(x, y, z, t)$
[37]	Hirota's method and ansatz method	**Only for** $q(x, y, z, t)$: Multiple soliton solutions, lump solutions, breather wave solutions, kink solutions (by tanh method), periodic solution (by tan method), real and complex solutions as a ratio of trigonometric functions, ratio of hyperbolic functions, and ratio of exponential functions	Not available	Not available
[38]	Unified method and generalized Kudryashov method	**Only for** $q(x, y, z, t)$: Ratio of trigonometric functions, ratio of hyperbolic functions	Not available	Not available
[39]	Hirota bilinear method and ansatz method	**Only for** $q(x, y, z, t)$: Resonant X and Y-type solitons and hybrid solutions, lump-periodic solution and lump-stripe soliton solution	Not available	Not available
In this work	Improved generalized Riccati equation mapping method	$q(x, y, z, t)$ is obtained; then, reversing the transformation, $\left(u = \frac{\partial q}{\partial x}\right)$, $u(x, y, z, t)$ is found. **For** $u(x, y, z, t)$: Bright soliton, bright-dark soliton, singular soliton, hyperbolic functions, ratio of hyperbolic functions, rational solutions, exponential solutions, singular periodic solutions, real and complex ratio of trigonometric functions	Available	Available

This study is organized as follows: Section 2 presents the detailed procedure of the IGREM technique. Section 3 explains in detail the application of the IGREM technique to Eq (1.5) and the retrieved solutions of Eq (1.3). Section 4 details the steps and outputs of the stability analysis. Section 5 includes the visual illustrations of both the selected derived solutions with 2D, 3D, and density plots, and the stability analysis results in 2D and 3D plots. Section 6 presents the study findings.

2. IGREM technique framework

The detailed procedure of the IGREM technique [40,43] for retrieving analytic solutions to NPDEs is explained as follows:

Assume the general NPDE:

$$S(h,\, h_x,\, h_y,\, h_z,\, h_t,\, h_{xx},\, h_{yy},\, h_{zz},\, h_{tt}, ...) = 0, \tag{2.1}$$

where $h(x,\, y,\, z,\, t)$ is the analytic solution for Eq (2.1).

1) Applying the wave transformation

$$h(x,\, y,\, z,\, t) = K(\mu), \quad \mu = \rho_1 t + \rho_2 x + \rho_3 y + \rho_4 z, \tag{2.2}$$

to Eq (2.1) transforms it to:

$$S(K,\, K',\, K'',\, K''',\, ...) = 0, \tag{2.3}$$

where S is a function in $K,\, K' = \dfrac{dK}{d\mu},\, K'' = \dfrac{d^2K}{d\mu^2}, ...\, etc.$

2) The solution to Eq (2.3) takes the following general form:

$$K(\mu) = \sum_{j=0}^{A} \tau_j\, \Omega^j(\mu), \quad \tau_A \neq 0, \tag{2.4}$$

where $\Omega(\mu)$ satisfies:

$$\Omega'(\mu) = \vartheta_0 + \vartheta_1\, \Omega(\mu) + \vartheta_2\, \Omega^2(\mu), \tag{2.5}$$

where A is an integer, $\tau_j\, (j = 0,\, 1,\, ..., A)$, $\vartheta_0,\, \vartheta_1$, and ϑ_2 are parameters to be determined.

3) A is determined by the balance between the nonlinearity and the dispersion in Eq (2.3).

4) Equation (2.3) is reduced to a polynomial in $\Omega(\mu)$ after the substitution of Eqs (2.4) and (2.5) in it.

5) All the coefficients of the generated polynomial in $\Omega(\mu)$ must vanish. This gives a system of equations in $\tau_j\, (j = 0,\, 1,\, ..., A)$, $\vartheta_0,\, \vartheta_1,\, \vartheta_2,\, \rho_1,\, \rho_2,\, \rho_3$, and ρ_4.

6) The generated system of equations is solved by proper software, such as Maple or Mathematica.

7) The following are the analytic solutions for Eq (2.5) with the arbitrary constants ξ, b_1, and b_2:

I) For $\psi = \vartheta_1^2 - 4\,\vartheta_0\,\vartheta_2 > 0$, $\vartheta_0\,\vartheta_2 \neq 0$, or $\vartheta_1\,\vartheta_2 \neq 0$, $b_1 \neq 0$, and $b_2 \neq 0$, hyperbolic solutions are:

$$\Omega_1(\mu) = -\frac{\sqrt{\psi}\, \tanh\left(\frac{\sqrt{\psi}(\mu+\xi)}{2}\right)}{2\,\vartheta_2} - \frac{\vartheta_1}{2\,\vartheta_2}, \tag{2.6}$$

$$\Omega_2(\mu) = -\frac{\sqrt{\psi}\, \coth\left(\frac{\sqrt{\psi}(\mu+\xi)}{2}\right)}{2\,\vartheta_2} - \frac{\vartheta_1}{2\,\vartheta_2}, \tag{2.7}$$

$$\Omega_3^{\pm}(\mu) = -\frac{\sqrt{\psi}\, \left(\tanh\left(\sqrt{\psi}\,(\mu+\xi)\right) \pm i\, \mathrm{sech}\left(\sqrt{\psi}\,(\mu+\xi)\right)\right)}{2\,\vartheta_2} - \frac{\vartheta_1}{2\,\vartheta_2}, \tag{2.8}$$

$$\Omega_4(\mu) = -\frac{\sqrt{\psi}\, \left(\tanh\left(\frac{\sqrt{\psi}(\mu+\xi)}{4}\right) + \coth\left(\frac{\sqrt{\psi}(\mu+\xi)}{4}\right)\right)}{4\,\vartheta_2} - \frac{\vartheta_1}{2\,\vartheta_2}, \tag{2.9}$$

$$\Omega_5^{\pm}(\mu) = \frac{\pm\,\sqrt{\psi\left(b_1^2+b_2^2\right)} - \sqrt{\psi}\,b_1\,\cosh\left(\sqrt{\psi}\,(\mu+\xi)\right)}{2\,\vartheta_2\,\left(b_1\,\sinh\left(\sqrt{\psi}\,(\mu+\xi)\right)+b_2\right)} - \frac{\vartheta_1}{2\,\vartheta_2}, \tag{2.10}$$

$$\Omega_6^{\pm}(\mu) = \frac{2\,\vartheta_0\cosh\left(\sqrt{\psi}\,(\mu+\xi)\right)}{\sqrt{\psi}\,\sinh\left(\sqrt{\psi}\,(\mu+\xi)\right) - \vartheta_1\,\cosh\left(\sqrt{\psi}\,(\mu+\xi)\right) \pm\, i\,\sqrt{\psi}}, \tag{2.11}$$

$$\Omega_7^{\pm}(\mu) = \frac{2\,\vartheta_0\sinh\left(\sqrt{\psi}\,(\mu+\xi)\right)}{\sqrt{\psi}\,\cosh\left(\sqrt{\psi}\,(\mu+\xi)\right) - \vartheta_1\,\sinh\left(\sqrt{\psi}\,(\mu+\xi)\right) \pm\,\sqrt{\psi}}. \tag{2.12}$$

II) Trigonometric solutions for $\psi = \vartheta_1^2 - 4\,\vartheta_0\,\vartheta_2 < 0,\ \vartheta_0\,\vartheta_2 \neq 0,\ \text{or}\ \vartheta_1\,\vartheta_2 \neq 0$, and $b_1^2 - b_2^2 > 0$:

$$\Omega_8(\mu) = \frac{\sqrt{-\psi}\,\tan\left(\frac{\sqrt{-\psi}(\mu+\xi)}{2}\right)}{2\,\vartheta_2} - \frac{\vartheta_1}{2\,\vartheta_2}, \tag{2.13}$$

$$\Omega_9(\mu) = -\frac{\sqrt{-\psi}\,\cot\left(\frac{\sqrt{-\psi}(\mu+\xi)}{2}\right)}{2\,\vartheta_2} - \frac{\vartheta_1}{2\,\vartheta_2}, \tag{2.14}$$

$$\Omega_{10}^{\pm}(\mu) = \frac{\sqrt{-\psi}\,\left(\tan\left(\sqrt{-\psi}\,(\mu+\xi)\right) \pm \sec\left(\sqrt{-\psi}\,(\mu+\xi)\right)\right)}{2\,\vartheta_2} - \frac{\vartheta_1}{2\,\vartheta_2}, \tag{2.15}$$

$$\Omega_{11}(\mu) = \frac{\sqrt{-\psi}\,\left(\tan\left(\frac{\sqrt{-\psi}(\mu+\xi)}{4}\right) - \cot\left(\frac{\sqrt{-\psi}(\mu+\xi)}{4}\right)\right)}{4\,\vartheta_2} - \frac{\vartheta_1}{2\,\vartheta_2}, \tag{2.16}$$

$$\Omega_{12}^{\pm}(\mu) = \frac{\pm\,\sqrt{-\psi\left(b_1^2-b_2^2\right)} - \sqrt{-\psi}\,b_1\,\cos\left(\sqrt{-\psi}\,(\mu+\xi)\right)}{2\,\vartheta_2\,\left(b_1\,\sin\left(\sqrt{-\psi}\,(\mu+\xi)\right)+b_2\right)} - \frac{\vartheta_1}{2\,\vartheta_2}, \tag{2.17}$$

$$\Omega_{13}^{\pm}(\mu) = \frac{-2\,\vartheta_0\cos\left(\sqrt{-\psi}\,(\mu+\xi)\right)}{\sqrt{-\psi}\,\sin\left(\sqrt{-\psi}\,(\mu+\xi)\right) + \vartheta_1\,\cos\left(\sqrt{-\psi}\,(\mu+\xi)\right) \pm\,\sqrt{-\psi}}, \tag{2.18}$$

$$\Omega_{14}^{\pm}(\mu) = \frac{-2\,\vartheta_0\sin\left(\sqrt{-\psi}\,(\mu+\xi)\right)}{\vartheta_1\,\sin\left(\sqrt{-\psi}\,(\mu+\xi)\right) - \sqrt{-\psi}\,\cos\left(\sqrt{-\psi}\,(\mu+\xi)\right) \pm\,\sqrt{-\psi}}. \tag{2.19}$$

III) Exponential solutions:

(1) For $\vartheta_0 = \lambda\,\vartheta_1$, and $\vartheta_2 = 0$:

$$\Omega_{15}(\mu) = e^{\vartheta_1\,(\mu+\xi)} - \lambda. \tag{2.20}$$

(2) For $\vartheta_0 = 0,\ \vartheta_1 \neq 0$, and $\vartheta_2 \neq 0$:

$$\Omega_{16}(\mu) = -\frac{\vartheta_1\,\nu}{\vartheta_2\,\left(e^{-\vartheta_1\,(\mu+\xi)} + \nu\right)}, \tag{2.21}$$

$$\Omega_{17}(\mu) = -\frac{\vartheta_1\,e^{\vartheta_1\,(\mu+\xi)}}{\vartheta_2\,\left(e^{\vartheta_1\,(\mu+\xi)} + \nu\right)}. \tag{2.22}$$

IV) Rational solutions:

(1) For $\vartheta_0 = \vartheta_1 = 0$, and $\vartheta_2 \neq 0$:

$$\Omega_{18}^{\pm}(\mu) = \pm \frac{1}{\vartheta_2 (\mu + \xi)}. \tag{2.23}$$

(2) For $\vartheta_0 \neq 0$, $\vartheta_1 \neq 0$, and $\vartheta_2 = \frac{\vartheta_1^2}{4\vartheta_0}$:

$$\Omega_{19}(\mu) = -\frac{2\vartheta_0 (\vartheta_1 (\mu + \xi) + 2)}{\vartheta_1^2 (\mu + \xi)}. \tag{2.24}$$

8) Different forms of $\Omega(\mu)$ are inserted into Eq (2.4) and then into Eq (2.2) to generate the analytic solutions of Eq (2.1).

9) The IGREM technique's Bäcklund transformation:

The IGREM technique's Bäcklund transformation of Eq (2.5) is:

$$\Omega(\mu) = \frac{-\vartheta_0 D_1 + \vartheta_2 D_2 \Omega_n(\mu)}{\vartheta_1 D_1 + \vartheta_2 (D_2 + D_1 \Omega_n(\mu))}, \tag{2.25}$$

where Ω_n, $n = 1, 2, 3, ..., 19$ as listed in Eqs (2.6)–(2.24), with D_1 and D_2 as arbitrary constants. Equation (2.25) provides an abundant number of additional analytic solutions for Eq (2.1).

3. Application of the IGREM technique

3.1. Strategy

The IGREM technique, introduced in Section 2, is applied to the (3+1)-dimensional B-type Kadomtsev–Petviashvili equation in Eq (1.5).

1) Let the exact solution for Eq (1.5) be

$$q(x, y, z, t) = K(\mu), \quad \mu = \rho_1 t + \rho_2 x + \rho_3 y + \rho_4 z. \tag{3.1}$$

The substitution of Eq (3.1) into Eq (1.5) reduces it to

$$\begin{aligned} &\rho_2^6 K^{(6)}(\mu) - 5\rho_3\rho_2^3 K^{(4)}(\mu) - 5\rho_3^2 K''(\mu) + \rho_2 (\beta\rho_3 + \gamma\rho_4) K''(\mu) + 9\rho_1\rho_2 K''(\mu) \\ &+\rho_2^2 K''(\mu) (\alpha - 30\rho_3 K'(\mu)) + 45\rho_2^4 K'^2(\mu) K''(\mu) + 15\rho_2^5 \left(K^{(4)}(\mu) K'(\mu) + K^{(3)}(\mu) K''(\mu)\right) = 0. \end{aligned} \tag{3.2}$$

2) Assume $K(\mu)$ as

$$K(\mu) = \sum_{j=0}^{A} \tau_j \, \Omega(\mu), \quad \tau_A \neq 0. \tag{3.3}$$

3) The balancing of the dispersion and the nonlinear terms in Eq (3.2) gives $A = 1$. Hence,

$$K(\mu) = \tau_0 + \tau_1 \Omega(\mu), \ \tau_1 \neq 0. \tag{3.4}$$

4) Equations (3.4) and (2.5) are inserted into Eq (3.2) to generate a polynomial in $\Omega(\mu)$.
5) All the coefficients of the generated polynomial in $\Omega(\mu)$ are set to zero, producing the following system of equations:

$$\begin{aligned}
&\Omega^0\, coeff:\ \tau_1\vartheta_0\vartheta_1(\rho_2^2(\alpha-30\rho_3\tau_1\vartheta_0)+\rho_2(\beta\rho_3+\gamma\rho_4)+9\rho_1\rho_2-5\rho_3^2+30\rho_2^5\tau_1\vartheta_0\left(\vartheta_1^2+5\vartheta_0\vartheta_2\right)\\
&\qquad+45\rho_2^4\tau_1^2\vartheta_0^2+\rho_2^6\left(\vartheta_1^4+52\vartheta_0\vartheta_2\vartheta_1^2+136\vartheta_0^2\vartheta_2^2\right)-5\rho_3\rho_2^3\left(\vartheta_1^2+8\vartheta_0\vartheta_2\right)=0,\\
&\Omega^1 coeff:\ \tau_1(2\vartheta_0\vartheta_2(\rho_2^2(\alpha-30\rho_3\tau_1\vartheta_0)+\rho_2(\beta\rho_3+\gamma\rho_4)+9\rho_1\rho_2-5\rho_3^2+150\rho_2^5\tau_1\vartheta_0^2\vartheta_2\\
&\qquad+45\rho_2^4\tau_1^2\vartheta_0^2+136\rho_2^6\vartheta_0^2\vartheta_2^2-40\rho_3\rho_2^3\vartheta_0\vartheta_2)+\vartheta_1^2(\rho_2^2(\alpha-60\rho_3\tau_1\vartheta_0)+\rho_2(\beta\rho_3+\gamma\rho_4)\\
&\qquad+9\rho_1\rho_2-5\rho_3^2+630\rho_2^5\tau_1\vartheta_0^2\vartheta_2+135\rho_2^4\tau_1^2\vartheta_0^2+720\rho_2^6\vartheta_0^2\vartheta_2^2-110\rho_3\rho_2^3\vartheta_0\vartheta_2)\\
&\qquad+\vartheta_1^4\left(6\rho_2^5\vartheta_0(10\tau_1+19\rho_2\vartheta_2)-5\rho_2^3\rho_3\right)+\rho_2^6\vartheta_1^6)=0,\\
&\Omega^2 coeff:\ 3\tau_1\vartheta_1(\vartheta_2(\rho_2^2(\alpha-60\rho_3\tau_1\vartheta_0)+\rho_2(\beta\rho_3+\gamma\rho_4)+9\rho_1\rho_2-5\rho_3^2+290\rho_2^5\tau_1\vartheta_0\vartheta_1^2\\
&\qquad+135\rho_2^4\tau_1^2\vartheta_0^2+21\rho_2^6\vartheta_1^4-25\rho_3\rho_2^3\vartheta_1^2)+2\rho_2^3\vartheta_0\vartheta_2^2\left(-50\rho_3+285\rho_2^2\tau_1\vartheta_0+196\rho_2^3\vartheta_1^2\right)\\
&\qquad+5\rho_2^2\tau_1\vartheta_1^2\left(-2\rho_3+9\rho_2^2\tau_1\vartheta_0+2\rho_2^3\vartheta_1^2\right)+616\rho_2^6\vartheta_0^2\vartheta_2^3)=0,\\
&\Omega^3 coeff:\tau_1(2\vartheta_2^2(\alpha\rho_2^2+\rho_2(\beta\rho_3+\gamma\rho_4)+9\rho_1\rho_2-5\rho_3^2+7\rho_2^6\left(43\vartheta_1^4+256\vartheta_0\vartheta_2\vartheta_1^2+88\vartheta_0^2\vartheta_2^2\right)\\
&\qquad-25\rho_3\rho_2^3\left(5\vartheta_1^2+4\vartheta_0\vartheta_2\right))+45\rho_2^4\tau_1^2\left(\vartheta_1^4+12\vartheta_0\vartheta_2\vartheta_1^2+6\vartheta_0^2\vartheta_2^2\right)\\
&\qquad+30\rho_2^2\tau_1\vartheta_2\left(\rho_2^3\left(13\vartheta_1^4+96\vartheta_0\vartheta_2\vartheta_1^2+38\vartheta_0^2\vartheta_2^2\right)-4\rho_3\left(\vartheta_1^2+\vartheta_0\vartheta_2\right)\right))=0,\\
&\Omega^4 coeff:\ 75\rho_2^2\tau_1\vartheta_1\vartheta_2(\tau_1+2\rho_2\vartheta_2)\left(\rho_2^2\vartheta_1^2(3\tau_1+14\rho_2\vartheta_2)+\vartheta_2\left(\rho_2^2\vartheta_0(9\tau_1+28\rho_2\vartheta_2)-2\rho_3\right)\right)=0,\\
&\Omega^5 coeff:\ 15\rho_2^2\tau_1\vartheta_2^2(\tau_1+2\rho_2\vartheta_2)\left(\rho_2^2\vartheta_1^2(27\tau_1+112\rho_2\vartheta_2)+2\vartheta_2\left(\rho_2^2\vartheta_0(9\tau_1+28\rho_2\vartheta_2)-2\rho_3\right)\right)=0,\\
&\Omega^6 coeff:\ 315\rho_2^4\tau_1\vartheta_1\vartheta_2^3(\tau_1+2\rho_2\vartheta_2)(\tau_1+4\rho_2\vartheta_2)=0,\\
&\Omega^7 coeff:\ 90\rho_2^4\tau_1\vartheta_2^4(\tau_1+2\rho_2\vartheta_2)(\tau_1+4\rho_2\vartheta_2)=0.
\end{aligned}\tag{3.5}$$

3.2. Solving the system of equations in Eq (3.5)

6) Mathematica software version 14 was used to solve the system of equations in Eq (3.5), under the following conditions: $\vartheta_2\neq 0,\ \rho_1\neq 0,\ \rho_2\neq 0,\ \rho_3\neq 0,$ and $\rho_4\neq 0$.

The imposed conditions are not arbitrary but arise naturally from the mathematical formulation of the IGREM method and the physical interpretation of the obtained wave solutions. Specifically:

- The condition $\vartheta_2 \neq 0$ is an essential requirement of the auxiliary Riccati equation used in the IGREM technique. If $\vartheta_2 = 0$, the Riccati equation degenerates into a simpler form, and the corresponding solution families derived in the present work no longer exist.
- The condition $\rho_1 \neq 0$ preserves the dependence of the traveling-wave variable on the temporal dimension.
- The condition $\rho_2 \neq 0$ ensures that the traveling-wave variable depends on the spatial coordinate x. Since the transformation $u = q_x$ is employed, setting $\rho_2 = 0$ would yield the trivial solution $u = 0$ and eliminate wave propagation in the principal direction.
- The condition $\rho_3 \neq 0$ guarantees genuine three-dimensional wave propagation by preserving the dependence of the traveling-wave variable on the $y-$ direction. When $\rho_3 = 0$, the solution reduces to a lower-dimensional special case, which is outside the scope of the present study.
- The condition $\rho_4 \neq 0$ guarantees genuine three-dimensional wave propagation by preserving the dependence of the traveling-wave variable on the $z-$ direction. When $\rho_4 = 0$, the solution reduces to a lower-dimensional special case, which is outside the scope of the present study.
- The discriminant $\psi = \vartheta_1^2 - 4\vartheta_0\vartheta_2$ determines the functional form of the obtained solutions. Specifically, $\psi > 0$ produces hyperbolic-function solutions, including bright, singular, and bright-dark solitons, whereas $\psi < 0$ generates trigonometric (singular-periodic) solutions. The limiting case $\psi = 0$ leads to rational solutions and is treated separately.

Two results were achieved by Mathematica software as follows:

3.2.1. Result 1

$$
\begin{aligned}
\tau_1 &= -4\,\rho_2\,\vartheta_2, \\
\rho_1 &= \frac{1}{9}\left(-\alpha\rho_2 - \beta\rho_2^3\left(\vartheta_1^2 - 4\vartheta_0\vartheta_2\right) - \gamma\,\rho_4 + 9\rho_2^5\left(\vartheta_1^2 - 4\vartheta_0\vartheta_2\right)^2\right), \\
\rho_3 &= \rho_2^3\left(\vartheta_1^2 - 4\vartheta_0\vartheta_2\right).
\end{aligned} \tag{3.6}
$$

The free parameters in this result are $\alpha,\ \beta,\ \gamma,\ \vartheta_0,\ \vartheta_1,\ \vartheta_2,\ \rho_2,$ and ρ_4.

- **Solution verification:**
  The solution is verified by direct substitution as follows:
  (1) The parameters from Eq (3.6) are inserted into Eqs (3.4) and (3.1), which yields

$$
q(x,\ y,\ z,\ t) = K(\mu) = \tau_0 - 4\,\rho_2\,\vartheta_2\,\Omega(\mu), \qquad \mu = \rho_1\,t + \rho_2\,x + \rho_3\,y + \rho_4\,z. \tag{3.7}
$$

  (2) The solution in Eq (3.7) and the parameters in Eq (3.6) are inserted into Eq (1.5), which reduces to

$$
\begin{aligned}
&-4\rho_2^7\,\vartheta_2\,[\Omega^{(6)}(\mu) - 5\Omega^{(4)}(\mu)\left(\vartheta_1^2 - 4\vartheta_2\,(\vartheta_0 - 3\Omega'(\mu))\right) \\
&+4\Omega''(\mu)\left(2\vartheta_2\vartheta_1^2\,(15\Omega'(\mu) - 4\vartheta_0) + \vartheta_2\left(4\vartheta_2\left(45\Omega'(\mu)^2 - 30\vartheta_0\Omega'(\mu) + 4\vartheta_0^2\right) - 15\Omega^{(3)}(\mu)) + \vartheta_1^4\right)\right] = 0.
\end{aligned} \tag{3.8}
$$

  (3) Using Eq (2.5), $\Omega'(\mu), \Omega''(\mu), ..., \Omega^{(6)}(\mu)$ are found and substituted in Eq (3.8), which yields an identity using Mathematica software as all $\Omega(\mu)$'s coefficients vanishes. Hence, $q(x,\ y,\ z,\ t)$ in Eq (3.7) is the exact solution for Eq (1.5).

- **The exact solution of the extended (3+1)-dimensional B-type Kadomtsev–Petviashvili equation in Eq (1.3):**
  The exact solution $u(x, y, z, t)$ of Eq (1.3) is found by the application of the transformation in Eq (1.4) to Eq (3.7) as follows:

$$u(x, y, z, t) = \frac{\partial q(x, y, z, t)}{\partial x} = -4\rho_2^2\,\vartheta_2\,\Omega'(\mu), \tag{3.9}$$

which, with the aid of Eq (2.5), reduces to

$$u(x, y, z, t) = -4\rho_2^2\,\vartheta_2\left(\vartheta_0 + \vartheta_1\,\Omega(\mu) + \vartheta_2\,\Omega^2(\mu)\right), \qquad \mu = \rho_1\,t + \rho_2\,x + \rho_3\,y + \rho_4\,z. \tag{3.10}$$

7) The insertion of different forms of $\Omega(\mu)$ from Eqs (2.6)–(2.24) into Eq (3.10) generates the following different forms of the derived analytic solutions for the extended (3+1)-dimensional B-type Kadomtsev–Petviashvili equation in Eq (1.3):

i) For $\psi = \vartheta_1^2 - 4\vartheta_0\vartheta_2 > 0, \vartheta_0\,\vartheta_2 \neq 0,$ or $\vartheta_1\,\vartheta_2 \neq 0$, $b_1 \neq 0$, and $b_2 \neq 0$, bright, singular, bright-dark solitons, and hyperbolic solutions. The singular solutions are valid on intervals excluding the singular points where the denominator of the solution vanishes:

$$u_{1.1,1}(x, y, z, t) = \rho_2^2\,\psi\,\mathrm{sech}^2\left(\frac{1}{2}\sqrt{\psi}\,(\xi + \rho_1 t + \rho_2 x + \rho_3 y + \rho_4 z)\right), \tag{3.11}$$

$$u_{1.1,2}(x, y, z, t) = -\rho_2^2\,\psi\,\mathrm{csch}^2\left(\frac{1}{2}\sqrt{\psi}\,(\xi + \rho_1 t + \rho_2 x + \rho_3 y + \rho_4 z)\right), \tag{3.12}$$

$$\begin{aligned} u^{\pm}_{1.1,3}(x, y, z, t) &= 2\rho_2^2\,\psi\,\mathrm{sech}^2\left(\sqrt{\psi}\,(\xi + \rho_1 t + \rho_2 x + \rho_3 y + \rho_4 z)\right) \\ &\mp 2\,i\,\rho_2^2\,\psi\,\tanh\left(\sqrt{\psi}\,(\xi + \rho_1 t + \rho_2 x + \rho_3 y + \rho_4 z)\right)\mathrm{sech}\left(\sqrt{\psi}\,(\xi + \rho_1 t + \rho_2 x + \rho_3 y + \rho_4 z)\right), \end{aligned} \tag{3.13}$$

$$\begin{aligned} u_{1.1,4}(x, y, z, t) &= \rho_2^2\,\psi - \frac{\rho_2^2\,\psi}{4} \\ &* \left(\tanh\left(\frac{1}{4}\sqrt{\psi}\,(\xi + \rho_1 t + \rho_2 x + \rho_3 y + \rho_4 z)\right) + \coth\left(\frac{1}{4}\sqrt{\psi}\,(\xi + \rho_1 t + \rho_2 x + \rho_3 y + \rho_4 z)\right)\right)^2, \end{aligned} \tag{3.14}$$

$$\begin{aligned} u^{\pm}_{1.1,5}(x, y, z, t) &= \frac{2b_1\rho_2^2\psi}{\left(b_1\sinh\left(\sqrt{\psi}\,(\xi + \rho_1 t + \rho_2 x + \rho_3 y + \rho_4 z)\right) + b_2\right)^2} \\ &* \{b_2\sinh\left(\sqrt{\psi}\,(\xi + \rho_1 t + \rho_2 x + \rho_3 y + \rho_4 z)\right) \\ &\pm \sqrt{b_1^2 + b_2^2}\cosh\left(\sqrt{\psi}\,(\xi + \rho_1 t + \rho_2 x + \rho_3 y + \rho_4 z)\right) - b_1\}, \end{aligned} \tag{3.15}$$

$$\begin{aligned} &u^{+}_{1.1,6}(x, y, z, t) = \\ &-\frac{4\rho_2^2\,\psi\,\vartheta_0\,\vartheta_2}{\left(\sqrt{\psi}\cosh\left(\frac{1}{2}\sqrt{\psi}\,(\xi + \rho_1 t + \rho_2 x + \rho_3 y + \rho_4 z)\right) - \vartheta_1\sinh\left(\frac{1}{2}\sqrt{\psi}\,(\xi + \rho_1 t + \rho_2 x + \rho_3 y + \rho_4 z)\right)\right)^2}, \end{aligned} \tag{3.16}$$

$$u^{-}_{1.1,6}(x,\ y,\ z,\ t) = \frac{4\,\rho_2^2\,\psi\,\vartheta_0\,\vartheta_2}{\left(\sqrt{\psi}\sinh\left(\frac{1}{2}\sqrt{\psi}\,(\xi+\rho_1 t+\rho_2 x+\rho_3 y+\rho_4 z)\right)-\vartheta_1\cosh\left(\frac{1}{2}\sqrt{\psi}\,(\xi+\rho_1 t+\rho_2 x+\rho_3 y+\rho_4 z)\right)\right)^2}. \tag{3.17}$$

ii) Singular periodic solutions for $\psi = \vartheta_1^2 - 4\,\vartheta_0\,\vartheta_2 < 0, \vartheta_0\,\vartheta_2 \neq 0,$ or $\vartheta_1\,\vartheta_2 \neq 0$, and $b_1^2 - b_2^2 > 0$. The singular-periodic solutions are defined over periodic intervals with isolated singularities:

$$u_{1.2,1}(x,\ y,\ z,\ t) = \rho_2^2\,\psi\ \sec^2\left(\frac{1}{2}\sqrt{-\psi}\,(\xi+\rho_1 t+\rho_2 x+\rho_3 y+\rho_4 z)\right), \tag{3.18}$$

$$u_{1.2,2}(x,\ y,\ z,\ t) = \rho_2^2\,\psi\ \csc^2\left(\frac{1}{2}\sqrt{-\psi}\,(\xi+\rho_1 t+\rho_2 x+\rho_3 y+\rho_4 z)\right), \tag{3.19}$$

$$u^{\pm}_{1.2,3}(x,\ y,\ z,\ t) = \frac{2\rho_2^2\psi}{1\mp\ \sin\left(\sqrt{-\psi}\,(\xi+\rho_1 t+\rho_2 x+\rho_3 y+\rho_4 z)\right)}, \tag{3.20}$$

$$u_{1.2,4}(x,\ y,\ z,\ t) = \ \psi\,\rho_2^2\ \csc^2\left(\frac{1}{2}\sqrt{-\psi}\,(\xi+\rho_1 t+\rho_2 x+\rho_3 y+\rho_4 z)\right), \tag{3.21}$$

$$\begin{aligned} u^{\pm}_{1.2,5}(x,\ y,\ z,\ t) &= \frac{2b_1\rho_2^2\psi}{\left(b_1\sin\left(\sqrt{-\psi}\,(\xi+\rho_1 t+\rho_2 x+\rho_3 y+\rho_4 z)\right)+b_2\right)^2} \\ &* \{b_2\sin\left(\sqrt{-\psi}\,(\xi+\rho_1 t+\rho_2 x+\rho_3 y+\rho_4 z)\right) \\ &\mp\sqrt{b_1^2-b_2^2}\cos\left(\sqrt{-\psi}\,(\xi+\rho_1 t+\rho_2 x+\rho_3 y+\rho_4 z)\right)+b_1\}, \end{aligned} \tag{3.22}$$

$$u^{\pm}_{1.2,6}(x,\ y,\ z,\ t) = \frac{\pm\,8\,\rho_2^2\,\psi\,\vartheta_0\,\vartheta_2\,\left(\sin\left(\sqrt{-\psi}\,(\xi+\rho_1 t+\rho_2 x+\rho_3 y+\rho_4 z)\right)\pm 1\right)}{\left(\sqrt{-\psi}\left(\sin\left(\sqrt{-\psi}\,(\xi+\rho_1 t+\rho_2 x+\rho_3 y+\rho_4 z)\right)\pm 1\right)+\vartheta_1\cos\left(\sqrt{-\psi}\,(\xi+\rho_1 t+\rho_2 x+\rho_3 y+\rho_4 z)\right)\right)^2}, \tag{3.23}$$

$$u^{+}_{1.2,7}(x,\ y,\ z,\ t) = \frac{4\,\rho_2^2\,\psi\,\vartheta_0\,\vartheta_2}{\left(\sqrt{-\psi}\sin\left(\frac{1}{2}\sqrt{h}\,(\xi+\rho_1 t+\rho_2 x+\rho_3 y+\rho_4 z)\right)+\vartheta_1\cos\left(\frac{1}{2}\sqrt{-\psi}\,(\xi+\rho_1 t+\rho_2 x+\rho_3 y+\rho_4 z)\right)\right)^2}, \tag{3.24}$$

$$u^{-}_{1.2,7}(x,\ y,\ z,\ t) = \frac{4\,\rho_2^2\,\psi\,\vartheta_0\,\vartheta_2}{\left(\sqrt{-\psi}\cos\left(\frac{1}{2}\sqrt{-\psi}\,(\xi+\rho_1 t+\rho_2 x+\rho_3 y+\rho_4 z)\right)-\vartheta_1\sin\left(\frac{1}{2}\sqrt{-\psi}\,(\xi+\rho_1 t+\rho_2 x+\rho_3 y+\rho_4 z)\right)\right)^2}. \tag{3.25}$$

iii) Exponential solutions:
For $\vartheta_0 = 0,\ \vartheta_1 \neq 0,\ \vartheta_2 \neq 0$, and v as an arbitrary constant:

$$u_{1.3,1}(x,\ y,\ z,\ t) = \frac{4\rho_2^2 v\vartheta_1^2 e^{\vartheta_1(\xi+\rho_1 t+\rho_2 x+\rho_3 y+\rho_4 z)}}{\left(v e^{\vartheta_1(\xi+\rho_1 t+\rho_2 x+\rho_3 y+\rho_4 z)}+1\right)^2}, \tag{3.26}$$

$$u_{1.3,2}(x,\ y,\ z,\ t) = \frac{4\rho_2^2 v \vartheta_1^2 e^{\vartheta_1(\xi+\rho_1 t+\rho_2 x+\rho_3 y+\rho_4 z)}}{\left(e^{\vartheta_1(\xi+\rho_1 t+\rho_2 x+\rho_3 y+\rho_4 z)}+v\right)^2}. \tag{3.27}$$

3.2.2. Result 2

$$\begin{aligned}\tau_1 &= -2\rho_2\vartheta_2,\\ \rho_1 &= -\frac{1}{9}\left(\alpha\rho_2+\beta\rho_3+\gamma\rho_4-\frac{5\rho_3^2}{\rho_2}+\rho_2^5\left(\vartheta_1^2-4\vartheta_0\vartheta_2\right)^2-5\rho_3\rho_2^2\left(\vartheta_1^2-4\vartheta_0\vartheta_2\right)\right).\end{aligned} \tag{3.28}$$

The free parameters in this result are α, β, γ, ϑ_0, ϑ_1, ϑ_2, ρ_2, ρ_3, and ρ_4.

- **Solution verification:**
  The solution is verified by direct substitution as follows:
  (1) The parameters from Eq (3.28) are inserted into Eq (3.4) and (3.1), which yields

$$q(x,\ y,\ z,\ t) = K(\mu) = \tau_0 - 2\rho_2\vartheta_2\,\Omega(\mu), \qquad \mu = \rho_1 t+\rho_2 x+\rho_3 y+\rho_4 z. \tag{3.29}$$

  (2) The solution in Eq (3.29) and the parameters in Eq (3.28) are inserted into Eq (1.5), which reduces to

$$\begin{aligned}&2\rho_2^4\vartheta_2[-\rho_2^3\Omega^{(6)}(\mu)+5\rho_3\Omega^{(4)}(\mu)+\rho_2^3\vartheta_1^4\Omega''(\mu)-\vartheta_1^2\left(5\rho_3+8\rho_2^3\vartheta_0\vartheta_2\right)\Omega''(\mu)+16\rho_2^3\vartheta_0^2\vartheta_2^2\Omega''(\mu)\\ &+20\rho_3\vartheta_0\vartheta_2\Omega''(\mu)+30\rho_2^3\vartheta_2\Omega^{(4)}(\mu)\Omega'(\mu)+30\rho_2^3\vartheta_2\Omega^{(3)}(\mu)\Omega''(\mu)-180\rho_2^3\vartheta_2^2\Omega'(\mu)^2\Omega''(\mu)\\ &-60\rho_3\vartheta_2\Omega'(\mu)\Omega''(\mu)]=0.\end{aligned} \tag{3.30}$$

  (3) Using Eq (2.5), $\Omega'(\mu), \Omega''(\mu), ..., \Omega^{(6)}(\mu)$ are found and substituted in Eq (3.30), which yields an identity using Mathematica software as all $\Omega(\mu)$'s coefficients vanishes. Hence, $q(x,\ y,\ z,\ t)$ in Eq (3.29) is the exact solution for Eq (1.5).

- **The exact solution of the extended (3+1)-dimensional B-type Kadomtsev–Petviashvili equation in Eq (1.3)**:
  The exact solution $u(x,\ y,\ z,\ t)$ of Eq (1.3) is found by the application of the transformation in Eq (1.4) to Eq (3.29) as follows:

$$u(x,\ y,\ z,\ t) = \frac{\partial q(x,\ y,\ z,\ t)}{\partial x} = -2\rho_2^2\vartheta_2\,\Omega'(\mu), \tag{3.31}$$

  which, with the aid of Eq (2.5), reduces to

$$u(x,\ y,\ z,\ t) = -2\rho_2^2\vartheta_2\left(\vartheta_0+\vartheta_1\,\Omega(\mu)+\vartheta_2\,\Omega^2(\mu)\right), \qquad \mu = \rho_1 t+\rho_2 x+\rho_3 y+\rho_4 z. \tag{3.32}$$

8) The insertion of different forms of $\Omega(\mu)$ from Eqs (2.6)–(2.24) into Eq (3.32) generates the following different forms of the derived analytic solutions for the extended (3+1)-dimensional B-type Kadomtsev—Petviashvili equation in Eq (1.3):

i) For $\psi = \vartheta_1^2 - 4\vartheta_0\vartheta_2 > 0, \vartheta_0\vartheta_2 \neq 0,$ or $\vartheta_1\vartheta_2 \neq 0, b_1 \neq 0,$ and $b_2 \neq 0$, bright, singular, bright-dark solitons, and hyperbolic solutions. The singular solutions are valid on intervals excluding the singular points where the denominator of the solution vanishes:

$$u_{2.1,1}(x,\ y,\ z,\ t) = \frac{1}{2}\rho_2^2\psi\,\mathrm{sech}^2\left(\frac{1}{2}\sqrt{\psi}\,(\xi+\rho_1 t+\rho_2 x+\rho_3 y+\rho_4 z)\right), \tag{3.33}$$

$$u_{2.1,2}(x,\, y,\, z,\, t) = -\frac{1}{2}\rho_2^2\,\psi\,\mathrm{csch}^2\left(\frac{1}{2}\,\sqrt{\psi}\,(\xi+\rho_1 t+\rho_2 x+\rho_3 y+\rho_4 z)\right), \tag{3.34}$$

$$\begin{aligned} u^{\pm}_{2.1,3}(x,\, y,\, z,\, t) &= \rho_2^2\,\psi\,\mathrm{sech}^2\left(\sqrt{\psi}\,(\xi+\rho_1 t+\rho_2 x+\rho_3 y+\rho_4 z)\right) \\ &\mp i\,\rho_2^2\,\psi\,\tanh\left(\sqrt{\psi}\,(\xi+\rho_1 t+\rho_2 x+\rho_3 y+\rho_4 z)\right)\mathrm{sech}\left(\sqrt{\psi}\,(\xi+\rho_1 t+\rho_2 x+\rho_3 y+\rho_4 z)\right), \end{aligned} \tag{3.35}$$

$$u_{2.1,4}(x,\, y,\, z,\, t) = -\frac{1}{2}\rho_2^2\,\psi\,\mathrm{csch}^2\left(\frac{1}{2}\,\sqrt{\psi}\,(\xi+\rho_1 t+\rho_2 x+\rho_3 y+\rho_4 z)\right), \tag{3.36}$$

$$\begin{aligned} u^{\pm}_{2.1,5}(x,\, y,\, z,\, t) &= \frac{b_1\,\rho_2^2\,\psi}{\left(b_1\sinh\left(\sqrt{\psi}\,(\xi+\rho_1 t+\rho_2 x+\rho_3 y+\rho_4 z)\right)+b_2\right)^2} \\ &*\{b_2\sinh\left(\sqrt{\psi}\,(\xi+\rho_1 t+\rho_2 x+\rho_3 y+\rho_4 z)\right) \\ &\pm\sqrt{b_1^2+b_2^2}\cosh\left(\sqrt{\psi}\,(\xi+\rho_1 t+\rho_2 x+\rho_3 y+\rho_4 z)\right)-b_1\}, \end{aligned} \tag{3.37}$$

$$\begin{aligned} &u^{+}_{2.1,6}(x,\, y,\, z,\, t) = \\ &-\frac{2\,\rho_2^2\,\psi\,\vartheta_0\,\vartheta_2}{\left(\sqrt{\psi}\cosh\left(\frac{1}{2}\,\sqrt{\psi}\,(\xi+\rho_1 t+\rho_2 x+\rho_3 y+\rho_4 z)\right)-\vartheta_1\sinh\left(\frac{1}{2}\,\sqrt{\psi}\,(\xi+\rho_1 t+\rho_2 x+\rho_3 y+\rho_4 z)\right)\right)^2}, \end{aligned} \tag{3.38}$$

$$\begin{aligned} &u^{-}_{2.1,6}(x,\, y,\, z,\, t) = \\ &\frac{2\,\rho_2^2\,\psi\,\vartheta_0\,\vartheta_2}{\left(\sqrt{\psi}\sinh\left(\frac{1}{2}\,\sqrt{\psi}\,(\xi+\rho_1 t+\rho_2 x+\rho_3 y+\rho_4 z)\right)-\vartheta_1\cosh\left(\frac{1}{2}\,\sqrt{\psi}\,(\xi+\rho_1 t+\rho_2 x+\rho_3 y+\rho_4 z)\right)\right)^2}. \end{aligned} \tag{3.39}$$

ii) Singular periodic solutions for $\psi = \vartheta_1^2 - 4\,\vartheta_0\,\vartheta_2 < 0, \vartheta_0\,\vartheta_2 \neq 0,$ or $\vartheta_1\,\vartheta_2 \neq 0$, and $b_1^2 - b_2^2 > 0$. The singular-periodic solutions are defined over periodic intervals with isolated singularities:

$$u_{2.2,1}(x,\, y,\, z,\, t) = \frac{1}{2}\,\rho_2^2\,\psi\,\sec^2\left(\frac{1}{2}\,\sqrt{-\psi}\,(\xi+\rho_1 t+\rho_2 x+\rho_3 y+\rho_4 z)\right), \tag{3.40}$$

$$u_{2.2,2}(x,\, y,\, z,\, t) = \frac{1}{2}\,\rho_2^2\,\psi\,\csc^2\left(\frac{1}{2}\,\sqrt{-\psi}\,(\xi+\rho_1 t+\rho_2 x+\rho_3 y+\rho_4 z)\right), \tag{3.41}$$

$$u^{\pm}_{2.2,3}(x,\, y,\, z,\, t) = \frac{\rho_2^2\,\psi}{1\mp\sin\left(\sqrt{-\psi}\,(\xi+\rho_1 t+\rho_2 x+\rho_3 y+\rho_4 z)\right)}, \tag{3.42}$$

$$u_{2.2,4}(x,\, y,\, z,\, t) = \frac{1}{2}\,\rho_2^2\,\psi\,\csc^2\left(\frac{1}{2}\,\sqrt{-\psi}\,(\xi+\rho_1 t+\rho_2 x+\rho_3 y+\rho_4 z)\right), \tag{3.43}$$

$$u^{\pm}_{2.2,5}(x,\ y,\ z,\ t) = \frac{b_1\rho_2^2\psi}{\Big(b_1 \sin\Big(\sqrt{-\psi}\,(\xi+\rho_1 t+\rho_2 x+\rho_3 y+\rho_4 z)\Big)+b_2\Big)^2}$$

$$*\{b_2 \sin\Big(\sqrt{-\psi}\,(\xi+\rho_1 t+\rho_2 x+\rho_3 y+\rho_4 z)\Big) \tag{3.44}$$

$$\mp\sqrt{b_1^2-b_2^2}\cos\Big(\sqrt{-\psi}\,(\xi+\rho_1 t+\rho_2 x+\rho_3 y+\rho_4 z)\Big)+b_1\},$$

$u^{\pm}_{2.2,6}(x,\ y,\ z,\ t) =$

$$\frac{\pm 4\rho_2^2\,\psi\,\vartheta_0\,\vartheta_2\Big(\sin\Big(\sqrt{-\psi}\,(\xi+\rho_1 t+\rho_2 x+\rho_3 y+\rho_4 z)\Big)\pm 1\Big)}{\Big(\sqrt{-\psi}\Big(\sin\Big(\sqrt{-\psi}\,(\xi+\rho_1 t+\rho_2 x+\rho_3 y+\rho_4 z)\Big)\pm 1\Big)+\vartheta_1\cos\Big(\sqrt{-\psi}\,(\xi+\rho_1 t+\rho_2 x+\rho_3 y+\rho_4 z)\Big)\Big)^2}, \tag{3.45}$$

$u^{+}_{2.2,7}(x,\ y,\ z,\ t) =$

$$\frac{2\rho_2^2\,\psi\,\vartheta_0\,\vartheta_2}{\Big(\sqrt{-\psi}\sin\Big(\frac{1}{2}\sqrt{-\psi}\,(\xi+\rho_1 t+\rho_2 x+\rho_3 y+\rho_4 z)\Big)+\vartheta_1\cos\Big(\frac{1}{2}\sqrt{-\psi}\,(\xi+\rho_1 t+\rho_2 x+\rho_3 y+\rho_4 z)\Big)\Big)^2}, \tag{3.46}$$

$u^{-}_{2.2,7}(x,\ y,\ z,\ t) =$

$$\frac{2\rho_2^2\,\psi\,\vartheta_0\,\vartheta_2}{\Big(\sqrt{-\psi}\cos\Big(\frac{1}{2}\sqrt{-\psi}\,(\xi+\rho_1 t+\rho_2 x+\rho_3 y+\rho_4 z)\Big)-\vartheta_1\sin\Big(\frac{1}{2}\sqrt{-\psi}\,(\xi+\rho_1 t+\rho_2 x+\rho_3 y+\rho_4 z)\Big)\Big)^2}. \tag{3.47}$$

iii) Exponential solutions:
For $\vartheta_0 = 0,\ \vartheta_1 \neq 0,\ \vartheta_2 \neq 0,$ and v as an arbitrary constant:

$$u_{2.3,1}(x,\ y,\ z,\ t) = \frac{2\rho_2^2\,v\,\vartheta_1^2 e^{\vartheta_1(\xi+\rho_1 t+\rho_2 x+\rho_3 y+\rho_4 z)}}{\Big(ve^{\vartheta_1(\xi+\rho_1 t+\rho_2 x+\rho_3 y+\rho_4 z)}+1\Big)^2}, \tag{3.48}$$

$$u_{2.3,2}(x,\ y,\ z,\ t) = \frac{2\rho_2^2\,v\,\vartheta_1^2 e^{\vartheta_1(\xi+\rho_1 t+\rho_2 x+\rho_3 y+\rho_4 z)}}{\Big(e^{\vartheta_1(\xi+\rho_1 t+\rho_2 x+\rho_3 y+\rho_4 z)}+v\Big)^2}. \tag{3.49}$$

iv) Rational solutions:

For $(\vartheta_0 = 0,\ \vartheta_1 = 0,$ and $\vartheta_2 \neq 0)$ or $\left(\vartheta_0 \neq 0,\ \vartheta_1 \neq 0,\text{ and } \vartheta_2 = \dfrac{\vartheta_1^2}{4\vartheta_0}\right)$:

$$u_{2.4,1}(x,\ y,\ z,\ t) = -\frac{2\rho_2^2}{(\xi+\rho_1 t+\rho_2 x+\rho_3 y+\rho_4 z)^2}. \tag{3.50}$$

9) Bäcklund's formula in Eq (2.25) provides more different forms of solutions. Table 2 presents a classification summary of independent solution families derived in this work.

Table 2. Classification summary of independent solution families derived in this work.

Solution family	Representative equations	Generating condition	Characteristic features	Independent family
Bright soliton	(3.11), (3.33)	$\psi > 0$	Maximum positive centered amplitude intensity	Yes
Singular soliton	(3.12), (3.34)	$\psi > 0$	Centered infinite amplitude intensity	Yes
Bright-dark soliton	(3.13), (3.35)	$\psi > 0$	Combined bright and dark characteristics	Yes
Singular periodic solution	(3.18)–(3.25), (3.40)–(3.47)	$\psi < 0$	Periodic oscillatory nature with isolated singularities	Yes
Exponential solution	(3.26), (3.27), (3.48), (3.49)	$\psi = \vartheta_1^2$	Rapid initial growth (or decay) in wave's amplitude	Yes
Rational solution	(3.50)	$\psi = 0$	Sudden huge change in the wave's amplitude	Yes

4. Stability analysis

In the following section of the study, the stability analysis for Eq (1.5) is investigated by linear stability analysis. This investigation begins with the assumption of the steady-state solution of Eq (1.5); then, a disturbance influences the steady-state solution, and finally, the dispersive relation is derived [48–50].

4.1. Steps of the linear stability analysis

1) If Eq (1.5) has the steady-state solution

$$q = \sqrt{\mathcal{B}}, \tag{4.1}$$

where $\sqrt{\mathcal{B}}$ is a real constant amplitude known as the normalized power. The steady-state solution in Eq (4.1) must satisfy Eq (1.5).

2) If the solution in Eq (4.1) is influenced by a very small disturbance, the steady-state solution under disturbance can be formulated as

$$q(x, y, z, t) = R(x, y, z, t) + \sqrt{\mathcal{B}}, \tag{4.2}$$

where $R(x, y, z, t)$ is the disturbance's amplitude, and $| R(x, y, z, t) | << \sqrt{\mathcal{B}}$.

3) The substitution of the disturbed steady-state solution in Eq (4.2) into Eq (1.5), followed by a

linearization with respect to $R(x,\, y,\, z,\, t)$, yields

$$\begin{aligned}&\frac{\partial^6 R(x,\, y,\, z,\, t)}{\partial x^6} - 5\,\frac{\partial^4 R(x,\, y,\, z,\, t)}{\partial y\,\partial x^3} + \alpha\,\frac{\partial^2 R(x,\, y,\, z,\, t)}{\partial x^2} - 5\,\frac{\partial^2 R(x,\, y,\, z,\, t)}{\partial y^2} + \beta\,\frac{\partial^2 R(x,\, y,\, z,\, t)}{\partial y\,\partial x}\\ &\quad + \gamma\,\frac{\partial^2 R(x,\, y,\, z,\, t)}{\partial z\,\partial x} + 9\,\frac{\partial^2 R(x,\, y,\, z,\, t)}{\partial t\,\partial x} = 0.\end{aligned} \tag{4.3}$$

4) Let the solution of Eq (4.3) be of the form

$$R(x,\, y,\, z,\, t) = r_1\ e^{i(L_1\ x + L_2\ y + L_3\ z - \omega\ t)} + r_2\ e^{-i(L_1\ x + L_2\ y + L_3\ z - \omega\ t)}, \tag{4.4}$$

where L_1, L_2, and L_3 are the disturbance's wave numbers in x, y, and z directions, respectively. ω is the disturbance's frequency, and r_1, r_2 are constants.

5) The substitution of $R(x,\, y,\, z,\, t)$ from Eq (4.4) into Eq (4.3), followed by separating the coefficients of $e^{-i(L_1\ x + L_2\ y + L_3\ z - \omega\ t)}$, and $e^{i(L_1\ x + L_2\ y + L_3\ z - \omega\ t)}$, yields

$$\begin{aligned} r_1 U_1 + r_2 U_2 = 0,\\ r_1 U_3 + r_2 U_4 = 0,\end{aligned} \tag{4.5}$$

which is formulated in the matrix form

$$\begin{bmatrix} U_1 & U_2 \\ U_3 & U_4 \end{bmatrix} \begin{bmatrix} r_1 \\ r_2 \end{bmatrix} = \begin{bmatrix} 0 \\ 0 \end{bmatrix}. \tag{4.6}$$

where $U_1 = U_4 = \alpha L_1^2 + L_1\,(\beta L_2 + \gamma L_3 - 9\omega) + L_1^6 + 5L_2L_1^3 - 5L_2^2$, and $U_2 = U_3 = 0$.

6) The system of equations in Eq (4.6) has a nontrivial solution if the determinant $\begin{vmatrix} U_1 & U_2 \\ U_3 & U_4 \end{vmatrix} = 0$, which gives the following dispersion relation:

$$\omega(L_1,\, L_2,\, L_3) = \frac{1}{9}\left(\alpha L_1 + \beta L_2 + \gamma L_3 + L_1^5 + 5L_2L_1^2 - \frac{5L_2^2}{L_1}\right). \tag{4.7}$$

7) The stability of the disturbed solution in Eq (4.2) depends on the disturbance's frequency $\omega(L_1,\, L_2,\, L_3)$ as follows:

- When $\omega(L_1,\, L_2,\, L_3)$ is purely real, the exponent $(i\,\omega)$ in Eq (4.4) is imaginary, and hence, the disturbance is only oscilating without amplitude change. This is known as neutral stability [51].
- When $\omega(L_1,\, L_2,\, L_3)$ is purely imaginary, the exponent $(i\,\omega)$ in Eq (4.4) is real, and hence, the amplitude of the disturbed solution changes exponentially. This is known as purely exponential dynamics [52].
- When $\omega(L_1,\, L_2,\, L_3)$ has non-zero real and imaginary parts, the real part affects the oscillatory behavior of the solution, while, the imaginary part affects the amplitude dynamics [52].
- The dispersion relation in Eq (4.7) shows that the disturbance's frequency $\omega(L_1,\, L_2,\, L_3)$ is purely real for all real-valued parameters L_1, L_2, L_3, α, β, and γ provided that $L_1 \neq 0$. This indicates that the disturbed solution in Eq (4.2) is neutrally stable.

4.2. Stability analysis conclusion

For real-valued parameters L_1, L_2, L_3, α, β, and γ under the condition that $L_1 \neq 0$, the disturbed solution in Eq (4.2) demonstrates only oscillatory disturbances, indicating that Eq (1.5), and hence the (3+1)-dimensional B-type Kadomtsev–Petviashvili equation in Eq (1.3), provides stable wave propagation without modulation instability for any choice of the parameters.

5. Results and figures

The implementation of the IGREM technique on the extended (3+1)-dimensional B-type Kadomtsev–Petviashvili equation in Eq (1.3) retrieved abundant types of solutions. Subsection 5.1 presents the graphical illustration of selected retrieved solutions. In Subsection 5.2, the graphical illustration of the results of stability analysis is presented.

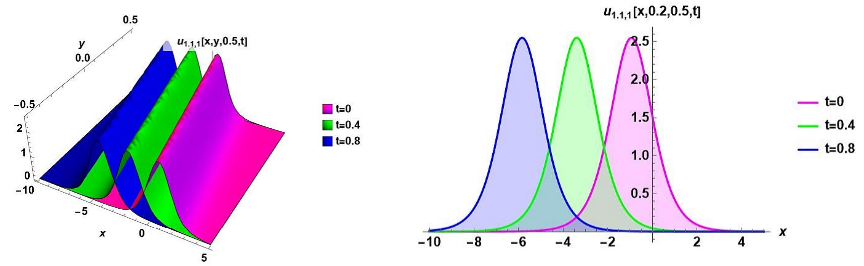

(a) 3D **(b)** 2D

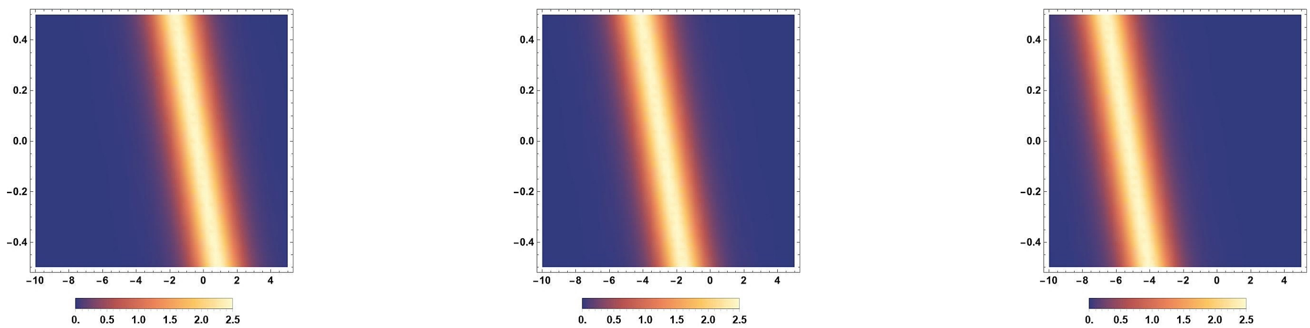

(c) Density plot at $t = 0$ **(d)** Density plot at $t = 0.4$ **(e)** Density plot at $t = 0.8$

Figure 1. The wave form of bright soliton $u_{1.1,1}(x, y, z, t)$ in Eq (3.11) with $\vartheta_0 = 0.5$, $\vartheta_1 = 2$, $\vartheta_2 = -0.6$, $\alpha = 0.9$, $\beta = 0.7$, $\gamma = 0.6$, $\xi = 0$, $\rho_2 = 0.7$, and $\rho_4 = 0.6$. (a) 3D wave form of $u_{1.1,1}(x, y, 0.5, t)$, which propagates in the negative x-axis direction. (b) Propagation of the wave form $u_{1.1,1}(x, 0.2, 0.5, t)$ as time increases; three shots are presented at $t = 0$, 0.4, and 0.8. (c)–(e) Corresponding density plots of (a), showing the wave spatiotemporal evolution with time.

5.1. Visual illustrations of some derived solutions

The derived solutions of Eq (1.3) included singular, bright-dark, and bright solitons, as well as rational, singular periodic, hyperbolic, and exponential solutions. The singular solutions are valid on intervals excluding the singular points where the denominator of the solution vanishes, while the singular-periodic solutions are defined over periodic intervals with isolated singularities. The dynamics of selected retrieved solutions are visually illustrated in Figures 1–6 by 2D, 3D, and density graphs.

Bright soliton $u_{1.1,1}(x, y, z, t)$ in Eq (3.11) is graphically illustrated by 2D, 3D, and density graphs in Figure 1. Bright solitons are characterized by a centered peak of maximum intensity. These solitons are crucial in optical communication systems because they can propagate over long distances without distortion, supporting high-speed data transmission efficiency. The 2D and 3D plots illustrate the stable propagation of bright solitons, emphasizing their role in maintaining signal integrity and enabling high-performance optical communication networks [43].

Singular soliton $|u_{1.1,2}(x, y, z, t)|$ in Eq (3.12) is graphically illustrated by 2D, 3D, and density graphs in Figure 2. Singular solitons feature a centered infinite amplitude and are valuable for studying extreme wave phenomena, aiding in the development of realistic models [43].

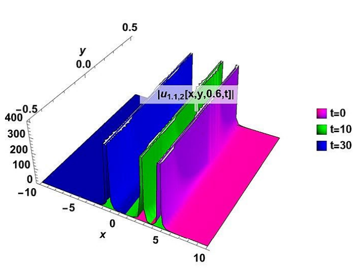

(a) 3D

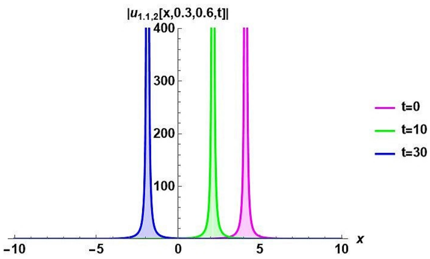

(b) 2D

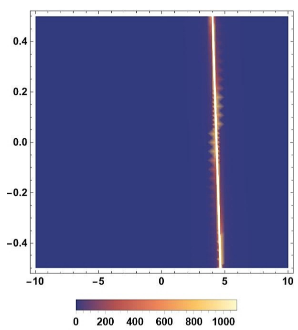

(c) Density plot at $t = 0$

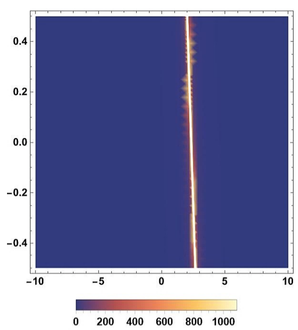

(d) Density plot at $t = 10$

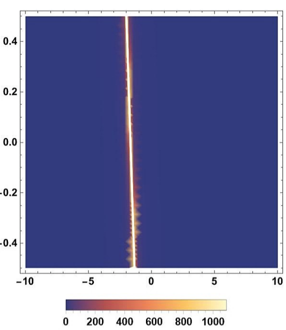

(e) Density plot at $t = 30$

Figure 2. The wave form of singular soliton $|u_{1.1,2}(x, y, z, t)|$ in Eq (3.12) with $\vartheta_0 = 2$, $\vartheta_1 = 3$, $\vartheta_2 = 1$, $\alpha = 0.7$, $\beta = 0.8$, $\gamma = 0.6$, $\xi = -4$, $\rho_2 = 0.8$, and $\rho_4 = 0.9$. (a) 3D wave form of $|u_{1.1,2}(x, y, 0.6, t)|$, which propagates in the negative x-axis direction. (b) Propagation of the wave form $|u_{1.1,2}(x, 0.3, 0.6, t)|$ as time increases; three shots are presented at $t = 0$, 10, and 30. (c)–(e) Corresponding density plots of (a), showing the wave spatiotemporal evolution with time.

Bright-dark soliton $Im[u^{-}_{1.1,3}(x, y, z, t)]$ in Eq (3.13) is graphically illustrated by 2D, 3D, and density graphs in Figure 3. The main characteristic of the combo bright-dark soliton is the presence of a wave packet that combines both the dark and bright solitons. The bright soliton presents a peak of the wave amplitude intensity, while the dark soliton presents a dip of the wave amplitude intensity, both coexisting within the same wave. The stability of this soliton is evident as they remain stable over long distances [53].

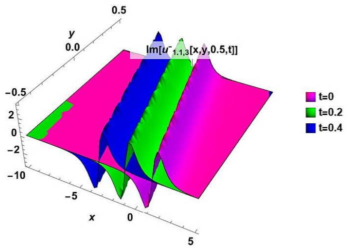

(a) 3D

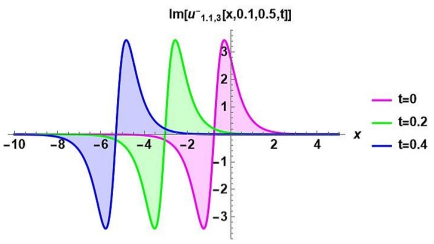

(b) 2D

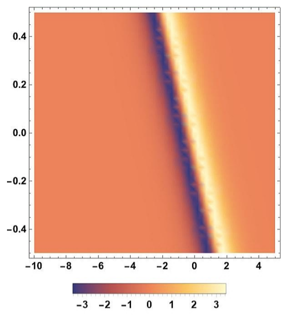

(c) Density plot at $t = 0$

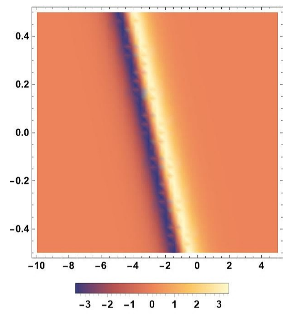

(d) Density plot at $t = 0.2$

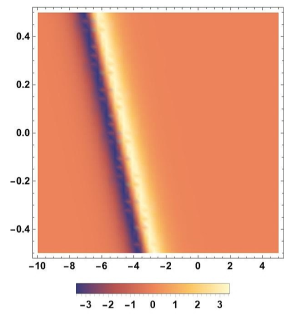

(e) Density plot at $t = 0.4$

Figure 3. The wave form of bright-dark soliton $Im[u^{-}_{1.1,3}(x, y, z, t)]$ in Eq (3.13) with $\vartheta_0 = 0.5$, $\vartheta_1 = 3$, $\vartheta_2 = 1$, $\alpha = 0.9$, $\beta = 0.7$, $\gamma = 0.6$, $\xi = 0$, $\rho_2 = 0.7$, and $\rho_4 = 0.6$. (a) 3D wave form of $Im[u^{-}_{1.1,3}(x, y, 0.5, t)]$, which propagates in the negative x-axis direction. (b) Propagation of the wave form $Im[u^{-}_{1.1,3}(x, 0.1, 0.5, t)]$ as time increases; three shots are presented at $t = 0$, 0.2, and 0.4. (c)–(e) Corresponding density plots of (a), showing the wave spatiotemporal evolution with time.

The singular periodic solution $|u_{1.2,1}(x, y, z, t)|$ in Eq (3.18) is graphically illustrated by 2D, 3D, and density graphs in Figure 4. Singular periodic solutions have significant applications in advanced signal processing techniques. The graphical representations demonstrate the oscillatory nature of these solutions, which can be exploited for pulse shaping, wavelength conversion, and other signal processing applications in optical communication systems [43].

The exponential solution $|u_{2.3,1}(x, y, z, t)|$ in Eq (3.48) is graphically illustrated by 2D, 3D, and density graphs in Figure 5. The main characteristic of the exponential solution is the rapid initial growth (or decay) in the wave amplitude at a rate proportional to the wave's current size. This solution plays an important role in studying systems with turbulence [49]. The exponential growth in ocean waves is driven by wind forcing and nonlinear interactions. The study of exponential growth is essential to understand how wind generates and builds waves from an initially calm water surface [43, 54, 55].

Rational solution $|u_{2.4,1}(x, y, z, t)|$ in Eq (3.50) is graphically illustrated by 2D, 3D, and density graphs in Figure 6. The main characteristic of the rational solution is the sudden huge change in the wave's amplitude. It is used to model the unexpected nonlinear wave phenomena in ocean known as rogue waves [56]. The graphical illustration of the rational solution shows its potential applications in the modeling of interactions of complex waves and in the optimization of signal transmission [43, 56].

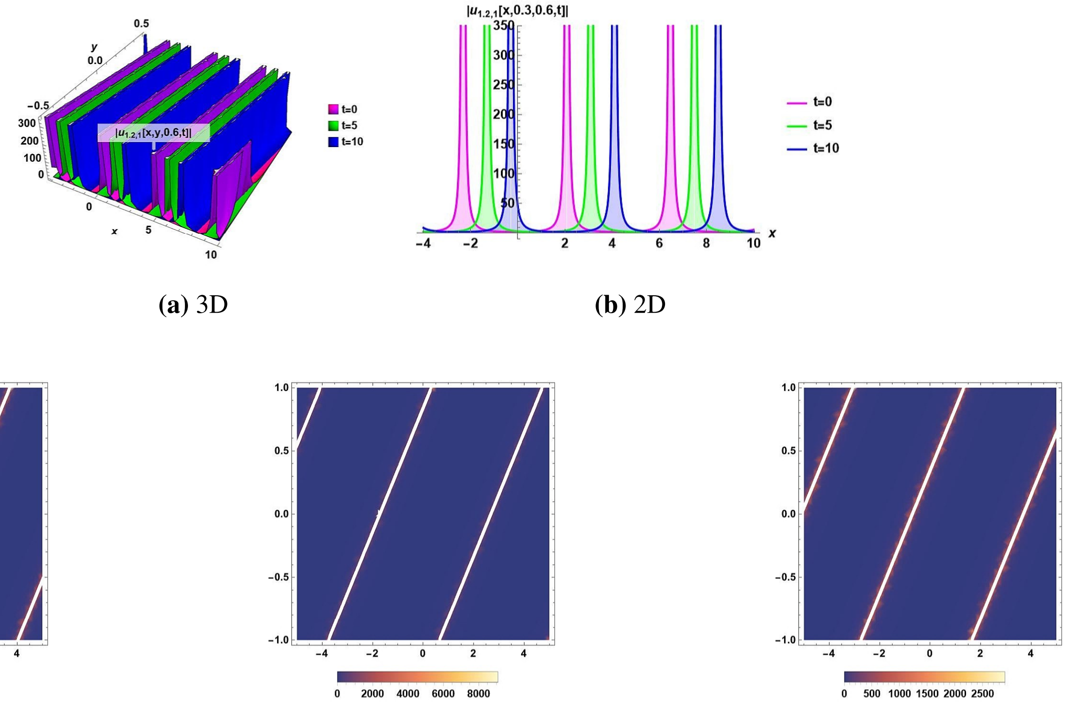

(a) 3D

(b) 2D

(c) Density plot at $t = 0$

(d) Density plot at $t = 5$

(e) Density plot at $t = 10$

Figure 4. The wave form of singular periodic solution $|u_{1.2,1}(x, y, z, t)|$ in Eq (3.18) with $\vartheta_0 = 1$, $\vartheta_1 = 0.9$, $\vartheta_2 = 1$, $\alpha = 0.6$, $\beta = 0.8$, $\gamma = 0.9$, $\xi = 0$, $\rho_2 = 0.8$, and $\rho_4 = 0.7$. (a) 3D wave form of $|u_{1.2,1}(x, y, 0.6, t)|$, which propagates in the positive x-axis direction. (b) Propagation of the wave form $|u_{1.2,1}(x, 0.3, 0.6, t)|$ as time increases; three shots are presented at $t = 0$, 5, and 10. (c)–(e) Corresponding density plots of (a), showing the wave spatiotemporal evolution with time.

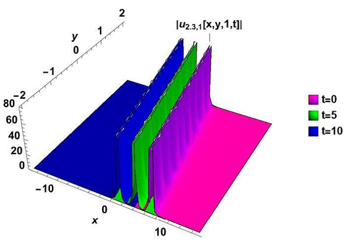

(a) 3D

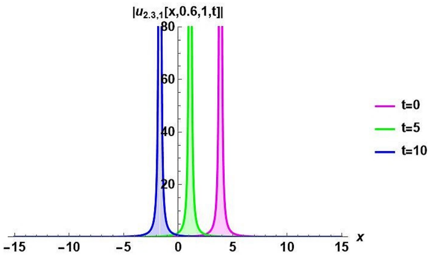

(b) 2D

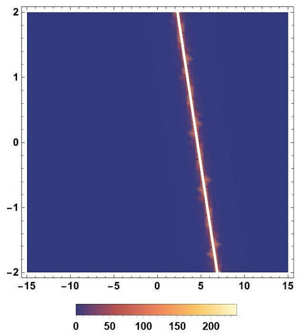

(c) Density plot at $t = 0$

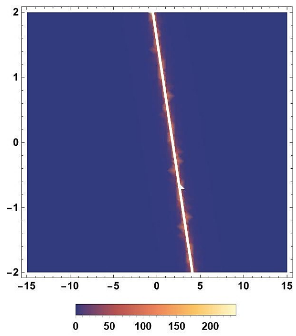

(d) Density plot at $t = 5$

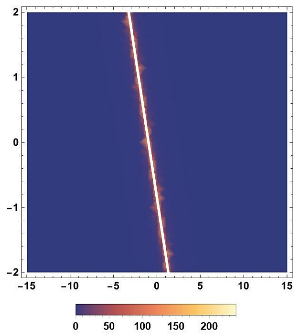

(e) Density plot at $t = 10$

Figure 5. The wave form of exponential solution $|u_{2.3,1}(x, y, z, t)|$ in Eq (3.48) with $v = -3$, $\vartheta_0 = 0$, $\vartheta_1 = 0.5$, $\vartheta_2 = 0.8$, $\alpha = 0.9$, $\beta = 0.7$, $\gamma = 0.6$, $\xi = -6$, $\rho_2 = 0.7$, $\rho_3 = 0.8$, and $\rho_4 = 0.6$. (a) 3D wave form of $|u_{2.3,1}(x, y, 1, t)|$, which propagates in the negative x-axis direction. (b) Propagation of the wave form $|u_{2.3,1}(x, 0.6, 1, t)|$ as time increases; three shots are presented at $t = 0$, 5, and 10. (c)–(e) Corresponding density plots of (a), showing the wave spatiotemporal evolution with time.

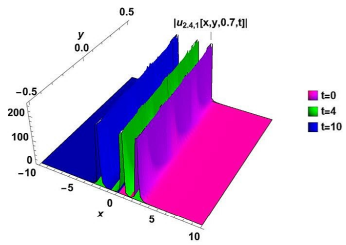

(a) 3D

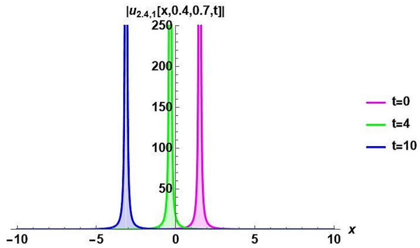

(b) 2D

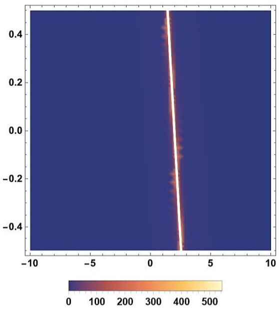

(c) Density plot at $t = 0$

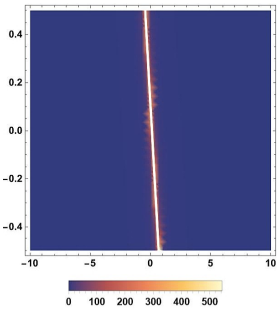

(d) Density plot at $t = 4$

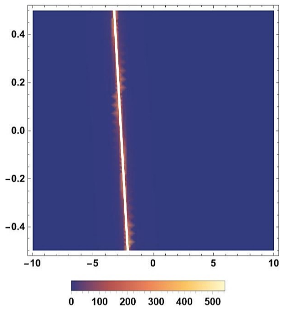

(e) Density plot at $t = 10$

Figure 6. The wave form of rational solution $|u_{2.4,1}(x, y, z, t)|$ in Eq (3.50) with $\vartheta_0 = 1$, $\vartheta_1 = 3$, $\alpha = 0.9$, $\beta = 0.7$, $\gamma = 0.6$, $\xi = -2$, $\rho_2 = 0.8$, $\rho_3 = 0.9$, and $\rho_4 = 0.6$. (a) 3D wave form of $|u_{2.4,1}(x, y, 0.7, t)|$, which propagates in the negative x-axis direction. (b) Propagation of the wave form $|u_{2.4,1}(x, 0.4, 0.7, t)|$ as time increases; three shots are presented at $t = 0$, 4, and 10. (c)–(e) Corresponding density plots of (a), showing the wave spatiotemporal evolution with time.

5.2. Visual illustration of stability analysis

- The 3-dimensional plot in Figure 7 (a) shows the variation of the frequency of disturbance $\omega(L_1, L_2, L_3)$ derived in Eq (4.7) against the wave numbers L_1 and L_2 for a constant value of the wave number L_3. The 2-dimensional plot in Figure 7 (b) shows the variation of the frequency of disturbance $\omega(L_1, L_2, L_3)$ against the disturbance wave number L_2 for three different values of the disturbance wave number $L_1 = \{-1, 0.5, 1\}$. Figure 7 (c) shows the variation of the frequency of disturbance $\omega(L_1, L_2, L_3)$ against the wave number L_1 for three different values of the disturbance wave number $L_2 = \{-1, 0.5, 1\}$.
- The 3-dimensional plot in Figure 8 (a) shows the variation of the frequency of disturbance $\omega(L_1, L_2, L_3)$ derived in Eq (4.7) against the wave numbers L_1 and L_3 for a constant value of the wave number L_2. The 2-dimensional plot in Figure 8 (b) shows the variation of the frequency of disturbance $\omega(L_1, L_2, L_3)$ against the disturbance wave number L_3 for three different values of the disturbance wave number $L_1 = \{-1, 0.5, 1\}$. Figure 8 (c) shows the variation of the frequency of disturbance $\omega(L_1, L_2, L_3)$ against the wave number L_1 for three different values of the disturbance wave number $L_3 = \{-1, 0.5, 1\}$.

- The 3-dimensional plot in Figure 9 (a) shows the variation of the frequency of disturbance $\omega(L_1, L_2, L_3)$ derived in Eq (4.7) against the wave numbers L_2 and L_3 for a constant value of the wave number L_1. The 2-dimensional plot in Figure 9 (b) shows the variation of the frequency of disturbance $\omega(L_1, L_2, L_3)$ against the disturbance wave number L_3 for three different values of the disturbance wave number $L_2 = \{-1, 0.5, 1\}$. Figure 9 (c) shows the variation of the frequency of disturbance $\omega(L_1, L_2, L_3)$ against the wave number L_2 for three different values of the disturbance wave number $L_3 = \{-1, 0.5, 1\}$.

  The conclusion from Figures 7–9 is that the disturbance frequency is stable unless near $L_1 = 0$, which is an asymptotic line. The frequency ω changes linearly w.r.t. L_3 and quadratically w.r.t. L_2.

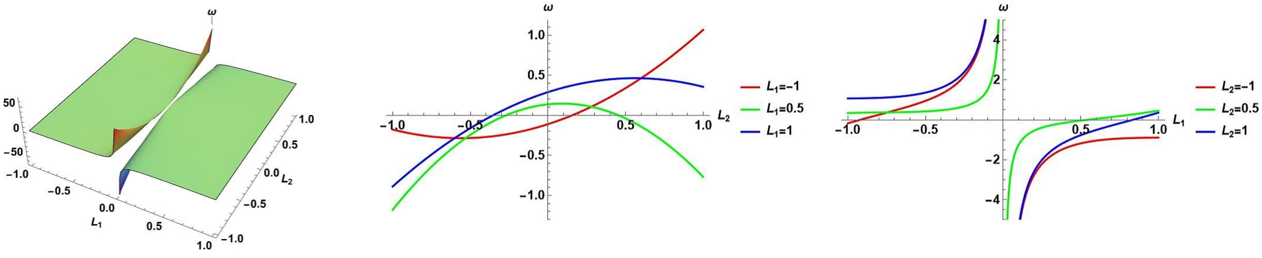

(a) **(b)** **(c)**

Figure 7. Profile of the disturbance frequency $\omega(L_1, L_2, L_3)$ in Eq (4.7) for $\alpha = 0.8, \beta = 0.6, \gamma = 0.9,$ and $L_3 = 0.9$. (a) 3D graph of $\omega(L_1, L_2, 0.9)$ versus L_1, L_2. (b) 2D graph of $\omega(L_1, L_2, 0.9)$ versus L_2 for $L_1 = \{-1, 0.5, 1\}$. (c) 2D graph of $\omega(L_1, L_2, 0.9)$ versus L_1 for $L_1 = \{-1, 0.5, 1\}$.

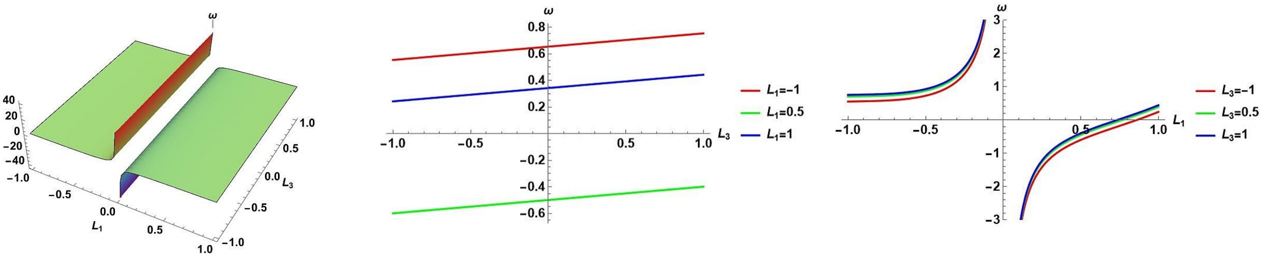

(a) **(b)** **(c)**

Figure 8. Profile of the disturbance frequency $\omega(L_1, L_2, L_3)$ in Eq (4.7) for $\alpha = 0.8, \beta = 0.6, \gamma = 0.9,$ and $L_2 = 0.8$. (a) 3D graph of $\omega(L_1, 0.8, L_3)$ versus L_1, L_3. (b) 2D graph of $\omega(L_1, 0.8, L_3)$ versus L_3 for $L_1 = \{-1, 0.5, 1\}$. (c) 2D graph of $\omega(L_1, 0.8, L_3)$ versus L_1 for $L_3 = \{-1, 0.5, 1\}$.

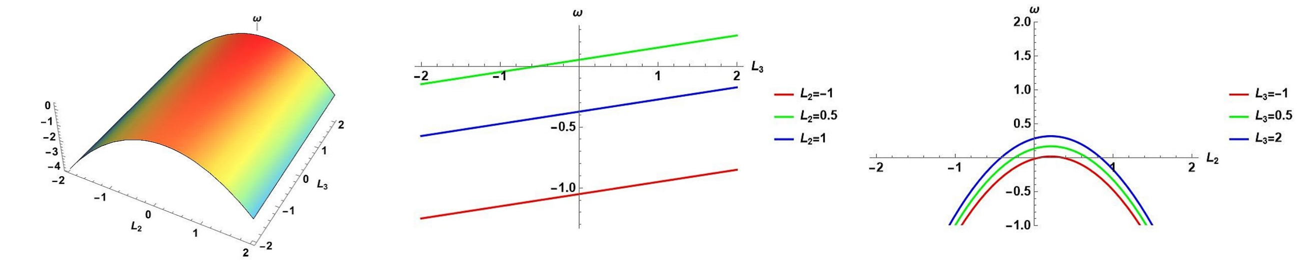

(a) **(b)** **(c)**

Figure 9. Profile of the disturbance frequency $\omega(L_1, L_2, L_3)$ in Eq (4.7) for $\alpha = 0.8$, $\beta = 0.6$, $\gamma = 0.9$, and $L_1 = 0.7$. (a) 3D graph of $\omega(0.7, L_2, L_3)$ versus L_2, L_3. (b) 2D graph of $\omega(0.7, L_2, L_3)$ versus L_3 for $L_2 = \{-1, 0.5, 1\}$. (c) 2D graph of $\omega(0.7, L_2, L_3)$ versus L_2 for $L_3 = \{-1, 0.5, 1\}$.

- The 2-dimensional plots in Figure 10 (a), (b), and (c) show the effect of the variation of parameters α, β, and γ, respectively, on the frequency of disturbance $\omega(L_1,\ 0.8,\ 0.9)$.
- The 2-dimensional plots in Figure 11 (a), (b), and (c) show the effect of the variation of parameters α, β, and γ, respectively, on the frequency of disturbance $\omega(0.7,\ L_2,\ 0.9)$.
- The 2-dimensional plots in Figure 12 (a), (b), and (c) show the effect of the variation of parameters α, β, and γ, respectively, on the frequency of disturbance $\omega(0.7,\ 0.8,\ L_3)$.

The conclusion from Figures 10–12 is that the relation between the disturbance's frequency ω and α is a direct relation for $L_1 > 0$ but is an inverse relation for $L_1 < 0$. Also, the relation between the disturbance's frequency ω and β is a direct relation for $L_2 > 0$ but is an inverse relation for $L_2 < 0$. And, the relation between the disturbance's frequency ω and γ is a direct relation for $L_3 > 0$ but is an inverse relation for $L_3 < 0$.

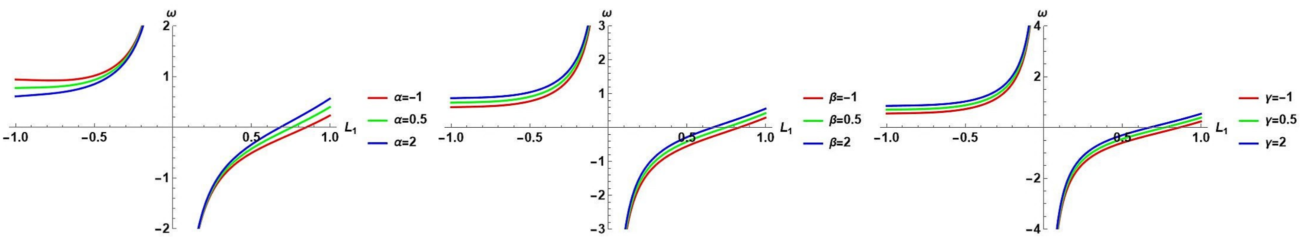

(a) **(b)** **(c)**

Figure 10. The effect of variation of the coefficients α, β, and γ in Eq (1.3) on the disturbance frequency $\omega(L_1, 0.8, 0.9)$ in Eq (4.7) versus the wave number in x−direction L_1. (a) For $\alpha = \{-1, 0.5, 2\}$, $\beta = 0.6$, and $\gamma = 0.9$. (b) For $\beta = \{-1, 0.5, 2\}$, $\alpha = 0.8$, and $\gamma = 0.9$. (c) For $\gamma = \{-1, 0.5, 2\}$, $\alpha = 0.8$, and $\beta = 0.6$.

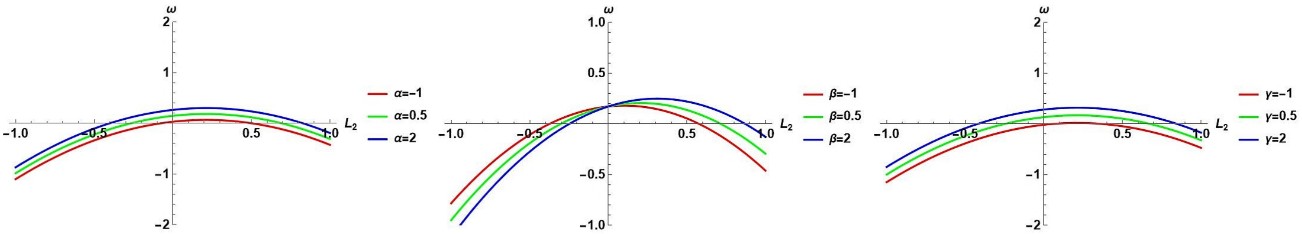

(a) **(b)** **(c)**

Figure 11. The effect of variation of the coefficients α, β, and γ in Eq (1.3) on the disturbance frequency $\omega(0.7, L_2, 0.9)$ in Eq (4.7) versus the wave number in $y-$direction L_2. (a) For $\alpha = \{-1, 0.5, 2\}$, $\beta = 0.6$, and $\gamma = 0.9$. (b) For $\beta = \{-1, 0.5, 2\}$, $\alpha = 0.8$, and $\gamma = 0.9$. (c) For $\gamma = \{-1, 0.5, 2\}$, $\alpha = 0.8$, and $\beta = 0.6$.

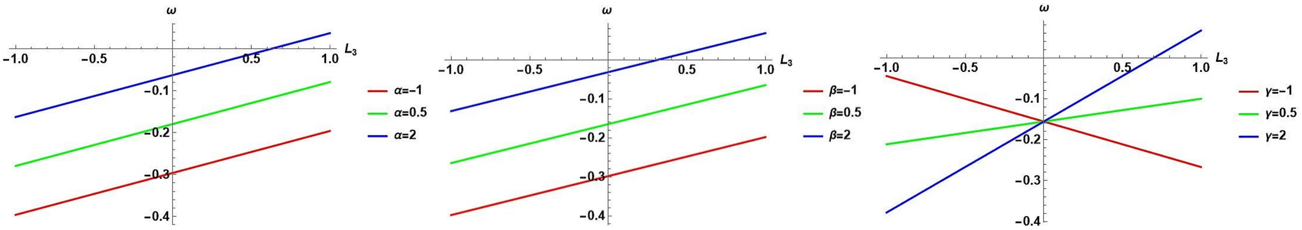

(a) **(b)** **(c)**

Figure 12. The effect of variation of the coefficients α, β, and γ in Eq (1.3) on the disturbance frequency $\omega(0.7, 0.8, L_3)$ in Eq (4.7) versus the wave number in $z-$direction L_3. (a) For $\alpha = \{-1, 0.5, 2\}$, $\beta = 0.6$, and $\gamma = 0.9$. (b) For $\beta = \{-1, 0.5, 2\}$, $\alpha = 0.8$, and $\gamma = 0.9$. (c) For $\gamma = \{-1, 0.5, 2\}$, $\alpha = 0.8$, and $\beta = 0.6$.

6. Conclusions

This study retrieved novel abundant exact solutions for the extended (3+1)-dimensional B-type Kadomtsev–Petviashvili equation (BKPE) in Eq (1.3) using the IGREM technique. The BKPE is of high importance in modeling nonlinear wave propagation in weakly dispersive media in fluid dynamics and plasmas. The IGREM technique succeeded to derive analytic solutions, such as singular, bright, and bright-dark solitons, as well as rational, singular periodic, exponential, and hyperbolic solutions. The verification steps of the solutions obtained in this study are presented in detail. In this work, the stability analysis for the equation under study was investigated using linear stability analysis, which proved that Eq (1.3) is neutrally stable with no existence of modulation instability for any choice of the system parameters. This is because the disturbance's frequency turned to be purely real-valued, which prohibited the exponential growth of any disturbances. 2D, 3D, and density plots were used for visual illustration of the dynamical behavior of some retrieved exact solutions of Eq (1.3) for the first time in the literature. Also, the 2D and 3D plots of the stability analysis were presented in this study for the first time in the literature. It is worth mentioning that throughout this work, the IGREM technique succeeded to achieve exact solutions, while both the ϕ^6, and the Sardar sub-equation methods failed to obtain any solution to the equation under study, as their constraints could not be satisfied. The limitations of the IGREM technique were the heavy symbolic computations and the inability to obtain solutions in terms of important functions such as Jacobi elliptic functions. In future work, it can be combined with other available techniques in the literature to overcome these limitations, while keeping its advantages to solve other complex structured NPDEs. Also, this work can be extended to fractional-order NPDEs.

Author contributions

Noha M. Kamel: Formal analysis, Software, Methodology, Writing-original draft, Visualization; Hamdy M. Ahmed: Validation, Supervision, Conceptualization, Writing-review & editing; Wafaa B. Rabie: Investigation, Writing-review & editing, Visualization.

Use of Generative-AI tools declaration

The authors declare that they have not used Artificial Intelligence tools in the creation of this article.

Conflict of interest

All authors declare no conflicts of interest in this paper.

References

1. H. Shao, S. Bilige, Dynamical asymptotic analysis to a (3+1)-dimensional B-type Kadomtsev–Petviashvili equation: The superposition formulas of rational solutions and interaction solutions under the bilinear vector method, *Math. Comput. Simulat.*, **240** (2026), 938–952. http://doi.org/10.1016/j.matcom.2025.07.058
2. H. Riaz, A. Farooq, Exact solutions and nonlinear wave interactions in a non-commutative coupled dispersionless system with variable coefficients, *Nonlinear Dyn.*, **113** (2025), 35125–35139. https://doi.org/10.1007/s11071-025-11833-6
3. H. W. A. Riaz, Quasi-Wronskian solitons in the non-commutative kuralay-IIA equation: analysis and simulations, *Phys. Scr.*, **100** (2025), 025239. http://doi.org/10.1088/1402-4896/ada4ee
4. H. W. A. Riaz, J. Lin, Darboux transformation for a semi-discrete matrix coupled dispersionless system, *Appl. Math. Lett.*, **158** (2024), 109217. http://doi.org/10.1016/j.aml.2024.109217
5. H. W. A. Riaz, A. Farooq, Hybrid analytical and neural-network approaches to the non-local short pulse equation, *Eur. Phys. J. C*, **85** (2025), 895. https://doi.org/10.1140/epjc/s10052-025-14634-8
6. W. Hereman, *Shallow water waves and solitary waves*, In: Mathematics of complexity and dynamical systems, New York: Springer, 2012, 1520–1532. http://doi.org/10.1007/978-1-4614-1806-1_96
7. W. B. Rabie, H. M. Ahmed, Diverse exact and solitary wave solutions to new extended KdV6 equation using IM extended tanh-function technique, *Pramana*, **98** (2024), 81. http://doi.org/10.1007/s12043-024-02767-6

8. S. A. Alkhateeb, S. Hussain, W. Albalawi, S. A. El-Tantawy, E. I. El-Awady, Dissipative Kawahara ion-acoustic solitary and cnoidal waves in a degenerate magnetorotating plasma, *J. Taibah Univ. Sci.*, **17** (2023), 2187606. http://doi.org/10.1080/16583655.2023.2187606

9. M. S. Tariq, W. Masood, M. Siddiq, S. Asghar, B. M. Alotaibi, S. M. E. Ismaeel, et al., Bäcklund transformation for analyzing a cylindrical Korteweg–de Vries equation and investigating multiple soliton solutions in a plasma, *Phys. Fluids*, **35** (2023), 103105. http://doi.org/10.1063/5.0166075

10. B. B. Kadomtsev, V. I. Petviashvili, On the stability of solitary waves in weakly dispersing media, *Dokl. Akad. Nauk SSSR*, **192** (1970), 753–756.

11. Y. Zhang, L. Gui, Inverse scattering transform for the two-dimensional B-type Kadomtsev–Petviashvili equation, *J. Comput. Appl. Math.*, **474** (2026), 117011. http://doi.org/10.1016/j.cam.2025.117011

12. A. Rahman, S. A. Khan, A. Qamar, Kadomtsev–Petviashvili equation for solitary waves in warm dense astrophysical electron-positron-ion plasmas, *Astrophys. Space Sci.*, **347** (2013), 119–127. http://doi.org/10.1007/s10509-013-1501-7

13. B. Sahu, N. K. Ghosh, Kadomstev-Petviashvili solitons in quantum plasmas, *Astrophys. Space Sci.*, **343** (2013), 289–292. http://doi.org/10.1007/s10509-012-1246-8

14. H. Berjamin, M. Destrade, G. Saccomandi, The KP equation of plane elastodynamics, *SIAM J. Appl. Math.*, **85** (2025), 1458–1474. http://doi.org/10.1137/24M1710036

15. S. V. Bulanov, P. V. Sasorov, F. Pegoraro, H. Kadlecová, S. S. Bulanov, T. Z. Esirkepov, et al., Electromagnetic solitons in quantum vacuum, *Phys. Rev. D*, **101** (2020), 016016. https://doi.org/10.1103/physrevd.101.016016

16. K. K. Ali, M. S. Mohamed, M. Maneea, A novel approach to q-fractional partial differential equations: Unraveling solutions through semi-analytical methods, *AIMS Mathematics*, **9** (2024), 33442–33466. http://doi.org/10.3934/math.20241596

17. Z. Li, M. Wu, E. Hussain, Y. Yildirim, Exactly explicit solutions of (2+1)-dimensional conformable fractional diffusive Predator–Prey model via neural networks method, *Front. Phys.*, **14** (2026), 1824530. http://doi.org/10.3389/fphy.2026.1824530

18. Z. Li, E. Hussain, Bifurcation analysis and chaotic behaviors of and a traveling-wave solution to the Zhiber–Shabat equation with a truncated M-fractional derivative, *Fractal Fract.*, **10** (2026), 335. https://doi.org/10.3390/fractalfract10050335

19. K. K. Ali, A. Wazwaz, M. Maneea, Efficient solutions for fractional Tsunami shallow-water mathematical model: A comparative study via semi analytical techniques, *Chaos Soliton. Fract.*, **178** (2024), 114347. http://doi.org/10.1016/j.chaos.2023.114347

20. N. Raza, A. Jhangeer, Z. Amjad, B. Rani, D. Baleanu, Exploring soliton dynamics and wave interactions in an extended Kadomtsev-Petviashvili-Boussinesq equation, *Ain Shams Eng. J.*, **16** (2025), 103395. http://doi.org/10.1016/j.asej.2025.103395

21. E. Date, M. Jimbo, M. Kashiwara, T. Miwa, Operator approach to the Kadomtsev–Petviashvili equation-transformation groups for soliton equations III, *J. Phys. Soc. Jap.*, **50** (1981), 3806–3812. https://doi.org/10.1143/JPSJ.50.3806

22. E. Date, M. Kashiwara, T. Miwa, Vertex operators and τ functions transformation groups for soliton equations, II, *Proc. Japan Acad. Ser. A Math. Sci.*, **57** (1981), 387–392. http://doi.org/10.3792/pjaa.57.387

23. E. Date, M. Jimbo, M. Kashiwara, T. Miwa, Transformation groups for soliton equations: IV. A new hierarchy of soliton equations of KP-type, *Physica D*, **4** (1982), 343–365. http://doi.org/10.1016/0167-2789(82)90041-0

24. X. Zhang, L. Wang, W. Chen, X. Yao, X. Wang, Y. Zhao, Dynamics of transformed nonlinear waves in the (3+1)-dimensional B-type Kadomtsev–Petviashvili equation I: Transitions mechanisms, *Commun. Nonlinear Sci.*, **105** (2022), 106070. http://doi.org/10.1016/j.cnsns.2021.106070

25. L. Feng, S. Tian, X. Wang, T. Zhang, Rogue waves, homoclinic breather waves and soliton waves for the (2+1)-dimensional B-type Kadomtsev–Petviashvili equation, *Appl. Math. Lett.*, **65** (2017), 90–97. http://doi.org/10.1016/j.aml.2016.10.009

26. A. Wazwaz, Breather wave solutions for an integrable (3+1)-dimensional combined pKP–BKP equation, *Chaos Soliton. Fract.*, **182** (2024), 114886. http://doi.org/10.1016/j.chaos.2024.114886

27. Y. Yuan, X. Zhao, Resonant solitons of the B-type Kadomtsev-Petviashvili equation, *Phys. Lett. A*, **458** (2023), 128592. https://doi.org/10.1016/j.physleta.2022.128592

28. M. H. Bashar, M. A. Mannaf, A. Rahman, M. S. Islam, H. Z. Mawa, P. Akter, Exploration of soliton solutions and bifurcation analysis in fluid dynamics governed by M fractional (3+1)-dimensional generalized B-type Kadomtsev–Petviashvili (gBKP) equation, *Eng. Rep.*, **8** (2026), e70642. http://doi.org/10.1002/eng2.70642

29. K. Wang, J. Liu, J. Si, G. Wang, Nonlinear dynamic behaviors of the (3+1)-dimensional B-type Kadomtsev–Petviashvili equation in fluid mechanics, *Axioms*, **12** (2023), 95. http://doi.org/10.3390/axioms12010095

30. C. Hu, B. Tian, X. Wu, Z. Du, X. Zhao, Lump wave-soliton and rogue wave-soliton interactions for a (3+1)-dimensional B-type Kadomtsev–Petviashvili equation in a fluid, *Chinese J. Phys.*, **56** (2018), 2395–2403. https://doi.org/10.1016/j.cjph.2018.06.021

31. A. Wazwaz, Two B-type Kadomtsev–Petviashvili equations of (2+1) and (3+1) dimensions: Multiple soliton solutions, rational solutions and periodic solutions, *Comput. Fluids*, **86** (2013), 357–362. http://doi.org/10.1016/j.compfluid.2013.07.028

32. J. Tu, S. Tian, M. Xu, P. Ma, T. Zhang, On periodic wave solutions with asymptotic behaviors to a (3+1)-dimensional generalized B-type Kadomtsev–Petviashvili equation in fluid dynamics, *Comput. Math. Appl.*, **72** (2016), 2486–2504. http://doi.org/10.1016/j.camwa.2016.09.003

33. F. Yuan, J. He, Y. Cheng, The degeneration of the breathers for the BKP equation, *Chinese J. Phys.*, **71** (2021), 190–201. http://doi.org/10.1016/j.cjph.2020.02.009

34. X. Wu, B. Tian, H. Chai, Y. Sun, Rogue waves and lump solutions for a (3+1)-dimensional generalized B-type Kadomtsev–Petviashvili equation in fluid mechanics, *Mod. Phys. Lett. B*, **31** (2017), 1750122. http://doi.org/10.1142/S0217984917501226

35. X. Yan, S. Tian, X. Wang, T. Zhang, Solitons to rogue waves transition, lump solutions and interaction solutions for the (3+1)-dimensional generalized B-type Kadomtsev–Petviashvili equation in fluid dynamics, *Int. J. Comput. Math.*, **96** (2018), 1839–1848. https://doi.org/10.1080/00207160.2018.1535708

36. C. Hu, B. Tian, X. Du, C. Zhang, Bright/dark breather-soliton, lump wave-soliton and rogue wave-soliton interactions for a (3+1)-dimensional generalized B-type Kadomtsev-Petviashvili equation in fluid mechanics, *Nonlinear Dyn.*, **108** (2022), 1585–1598. http://doi.org/10.1007/s11071-022-07204-0

37. A. M. Wazwaz, Study on a (3+1)-dimensional B-type Kadomtsev–Petviashvili equation in nonlinear physics: Multiple soliton solutions, lump solutions, and breather wave solutions, *Chaos Soliton. Fract.*, **189** (2024), 115668. http://doi.org/10.1016/j.chaos.2024.115668

38. M. Ekici, On solving the (3+1)-dimensional B-type Kadomtsev-Petviashvili equation by using two efficient method, *Süleyman Demirel Üniversitesi Fen Bilimleri Enstitüsü Dergisi*, **29** (2025), 54–61. http://doi.org/10.19113/sdufenbed.1611725

39. H. Alsaud, M. N. Rafiq, M. H. Rafiq, A novel investigation of the extended (3+1)-dimensional B-type Kadomtsev–Petviashvili equation: Analysis and simulations, *Int. J. Theor. Phys.*, **64** (2025), 216. http://doi.org/10.1007/s10773-025-06081-8

40. H. Ur Rehman, A. R. Seadawy, S. Razzaq, S. T. R. Rizvi, Optical fiber application of the improved generalized Riccati equation mapping method to the perturbed nonlinear Chen-Lee-Liu dynamical equation, *Optik*, **290** (2023), 171309. https://doi.org/10.1016/j.ijleo.2023.171309

41. M. Rani, N. Ahmed, S. S. Dragomir, S. T. Mohyud-Din, I. Khan, K. S. Nisar, Some newly explored exact solitary wave solutions to nonlinear inhomogeneous Murnaghan's rod equation of fractional order, *J. Taibah Univ. Sci.*, **15** (2021), 97–110. https://doi.org/10.1080/16583655.2020.1841472

42. B. Li, Y. Chen, H. Xuan, H. Zhang, Generalized Riccati equation expansion method and its application to the (3 + 1)-dimensional Jumbo–Miwa equation, *Appl. Math. Comput.*, **152** (2004), 581–595. http://doi.org/10.1016/S0096-3003(03)00578-2

43. N. M. Kamel, H. M. Ahmed, W. B. Rabie, Exploring novel soliton, wave solutions, and modulation instability analysis for the (3+1)-dimensional KP-SKR equation using the improved generalized Riccati equation mapping approach, *Sci. Rep.*, **15** (2025), 37741. http://doi.org/10.1038/s41598-025-22030-1

44. Y. Salathiel, Y. Amadou, G. Betchewe, S. Y. Doka, K. T. Crepin, Soliton solutions and traveling wave solutions for a discrete electrical lattice with nonlinear dispersion through the generalized Riccati equation mapping method, *Nonlinear Dyn.*, **87** (2017), 2435–2443. http://doi.org/10.1007/s11071-016-3201-7

45. S. Bibi, N. Ahmed, I. Faisal, S. T. Mohyud-Din, M. Rafiq, U. Khan, Some new solutions of the Caudrey–Dodd–Gibbon (CDG) equation using the conformable derivative, *Adv. Differ. Equ.*, **2019** (2019), 89. http://doi.org/10.1186/s13662-019-2030-7

46. M. Bilal, Y. M. Alawaideh, S. Ur Rehman, I. Popa, B. M. Al-khamiseh, H. Ghannam, Complex soliton wave patterns of Gross–Pitaevskii systems: Application in quantum and optical engineering, *Sci. Rep.*, **15** (2025), 44265. http://doi.org/10.1038/s41598-025-27902-0

47. A. Ankiewicz, M. Bokaeeyan, N. Akhmediev, Shallow-water rogue waves: An approach based on complex solutions of the Korteweg–de Vries equation, *Phys. Rev. E*, **99** (2019), 050201. http://doi.org/10.1103/PhysRevE.99.050201

48. N. Alam, M. S. Ullah, T. A. Nofal, H. M. Ahmed, K. K. Ahmed, M. A. Al-Nahhas, Novel dynamics of the fractional KFG equation through the unified and unified solver schemes with stability and multistability analysis, *Nonlinear Eng.*, **13** (2024), 20240034. https://doi.org/10.1515/nleng-2024-0034

49. N. M. Kamel, H. M. Ahmed, W. B. Rabie, Solitons unveilings and modulation instability analysis for sixth-order coupled nonlinear Schrödinger equations in fiber bragg gratings, *AIMS Mathematics*, **10** (2025), 6952–6980. http://doi.org/10.3934/math.2025318

50. N. M. Kamel, H. M. Ahmed, W. B. Rabie, Unveiling solitons and traveling wave solutions with modulation instability analysis for extended (3+1)-dimensional seventh-order standard Ito and modified Ito equations, *Ain Shams Eng. J.*, **16** (2025), 103475. http://doi.org/10.1016/j.asej.2025.103475

51. M. S. Ghayad, H. M. Ahmed, N. M. Badra, W. B. Rabie, Generation of multi-form exact wave solutions and linear stability analysis in the generalized (3+1)-D P-type plasma system using a modified extended mapping technique, *Sci. Rep.*, **16** (2026), 15173. http://doi.org/10.1038/s41598-026-49817-0

52. A. E. Rateb, H. M. Ahmed, A. Darwish, M. Ammar, W. B. Rabie, Analytical wave families and stability dynamics in a modified complex Ginzburg–Landau model via the modified extended direct algebraic method, *Sci. Rep.*, **16** (2026), 7485. http://doi.org/10.1038/s41598-026-37824-0

53. F. M. Omar, M. A. S. Murad, S. S. Mahmood, S. Malik, T. Radwan, Optical solitons, bifurcation, and chaos in the nonlinear conformable Schrödinger equation with group velocity dispersion coefficients and second-order spatiotemporal terms, *Sci. Rep.*, **15** (2025), 20073. http://doi.org/10.1038/s41598-025-04387-5

54. T. Li, L. Shen, Evolution of wave characteristics during wind-wave generation, 2022, arXiv: 2208.02489. https://doi.org/10.48550/arXiv.2208.02489

55. R. Wu, A. Guo, S. Zhu, J. Liu, Growth of wind-driven waves under uniform currents, *Coast. Eng.*, **198** (2025), 104704. http://doi.org/10.1016/j.coastaleng.2025.104704

56. B. D. V. Campos, Characterization of rational solutions of a KdV-like equation, *Math. Comput. Simulat.*, **201** (2022), 396–416. http://doi.org/10.1016/j.matcom.2022.05.022

AIMS Press

© 2026 the Author(s), licensee AIMS Press. This is an open access article distributed under the terms of the Creative Commons Attribution License (https://creativecommons.org/licenses/by/4.0)